

2002

Tectonic geomorphology of the Red Rock fault, segmentation and recent rupture history in the northern arm of the Yellowstone Topographic Lake

Nathan W. Harkins
Lehigh University

Follow this and additional works at: <http://preserve.lehigh.edu/etd>

Recommended Citation

Harkins, Nathan W., "Tectonic geomorphology of the Red Rock fault, segmentation and recent rupture history in the northern arm of the Yellowstone Topographic Lake" (2002). *Theses and Dissertations*. Paper 745.

This Thesis is brought to you for free and open access by Lehigh Preserve. It has been accepted for inclusion in Theses and Dissertations by an authorized administrator of Lehigh Preserve. For more information, please contact preserve@lehigh.edu.

Harkins, Nathan W.

Tectonic
Geomorphology of
the Red Rock
Fault,
Segmentation and
Recent Rupture...

January 2003

**Tectonic geomorphology of the Red Rock fault, segmentation and recent
rupture history in the northern arm of the Yellowstone Topographic Wake**

by

Nathan W. Harkins

A Thesis

Presented to the Graduate and Research Committee

of Lehigh University

in Candidacy for the Degree of

Master of Science

in

Geological Sciences

Lehigh University

December 5, 2002

This thesis is accepted and approved in partial fulfillment of the requirements for
the master of Science

12/04/02

Date

Dr. David Anastasio
Thesis Adviser

Dr. Frank Pazzaglia
committee member

Dr. Anne Metzger
Department Chairperson

ACKNOWLEDGEMENTS

This research was supported by DOI-USGS-EDMAP grant 01HQA0188 and The American Association of Petroleum Geologists Grants in Aid program. I would like to gratefully acknowledge the assistance of Diana Latta, who acted as a field assistant in southwest Montana, and the hospitality of Arlene Greensladd, who was extremely generous and helpful over two field seasons. I would also like to thank my advisor, Dave Anastasio, who was also my undergraduate advisor and continues to be a great mentor and friend. Thanks also to my committee members, Frank Pazzalgia and Edward Evenson. The research and paper have benefited from discussions with Jerry Bartholomew, Michael Stickney, and Kathy Haller. Finally I would like to thank my parents for everything.

TABLE OF CONTENTS

List of tables.....	v
List of figures.....	vi
Abstract.....	1
Introduction.....	2
Geologic Setting.....	4
Previous Work.....	7
Methods.....	8
Results.....	12
Discussion.....	17
Conclusion.....	25
Tables.....	28
Figure Captions.....	30
Figures.....	32
References.....	42
Appendix.....	48
Vita.....	66

LIST OF TABLES

Table 1. Drainage basin geomorphic indices..... 28

Table 2 Fan and terrace unit soil pit data.....29

LIST OF FIGURES

Figure 1. Map of the Yellowstone hot spot.....	32
Figure 2. Geologic map of the Red Rock fault.....	33
Figure 3. Map of Quaternary fan and terrace units along the Red Rock fault.....	34
Figure 4. Maps and cross-sections of various fan and terrace units.....	35
Figure 5. Select channel long profiles.....	36
Figure 6. Contour map of <i>SL</i> values within footwall basins.....	37
Figure 7. Footwall drainage basin hypsometric integral values.....	38
Figure 8. Basin volume and area geometries.....	39
Figure 9. Conceptual plot of relative index sensitivities.....	40
Figure 10. Shaded elevation map of the eastern Snake River Plain showing past hotspot eruptive centers and active faults...	41

ABSTRACT

The Red Rock fault, an east dipping range front normal fault in southwest Montana, displays significant recent offset and marked segmentation. Field characterization of soils coupled with numeric radiocarbon ages in offset footwall fans and terraces constrain the rupture history at a number of locations along strike. These data are coupled with morphometric analysis of dated alluvial fan deposits and adjacent 2nd and 3rd order footwall drainage basins to further constrain fault kinematics and segmentation. Three segments are recognized, the southernmost of which extends ~8 km and is the most recently active, displaying offset Holocene alluvial fan surfaces. The central segment, previously not recognized, extends for ~11 km and is characterized by offset of late Pleistocene fans and pronounced changes in footwall channel morphology. Extending ~8 km up to the northern terminus of the fault, the absence of surface ruptures in latest Pleistocene fan units along the northern segment indicate a lack of offset since the late middle Pleistocene. Surface rupture, hanging wall fan, and footwall drainage basin data sets are synthesized to demonstrate a displacement gradient along the Red Rock fault. These data suggest that the Red Rock fault has only recently shifted over to the characteristic kinematics indicated by the present pattern of segmentation. We use these results to further refine geomorphic criteria in the recognition and definition of fault segments. The displacement geometry and kinematic history of the Red Rock fault helps to define a time-transgressive sequence of fault development within range front normal faults north of the Snake River Plain, with a likely genetic link to the passage of the Yellowstone hot spot.

INTRODUCTION

The active, ongoing response of the crust and upper mantle to Yellowstone hot spot tectonism figures prominently in the tectonic and geomorphic evolution of the northern Rocky Mountains. A spatially persistent, high standing topographic swell wraps around the hotspot to the north, east, and south and has been described as a wake or wave by previous authors (e.g. Stickney and Bartholomew, 1987, Crone & Haller, 1991, Pierce and Morgan, 1992)(Figure 1). A halo of crustal deformation delineated by active normal faulting mirrors the distribution of the hot spot wake (e.g Anders et al., 1989, Smith et al., 1989, Rodgers et al., 1990, Parsons et al., 1994, McQuarrie and Rodgers, 1998). In the northern arm of the topographic wake, the most prominent physiographic manifestation of this active deformation are several active predominantly NW-SE striking normal faults and accompanying high standing footwall ranges that extend tens of kilometers north of the Snake River Plain. The genetic relationship of these faults to the hot spot system, however, remains speculative (e.g. Morgan, 1972, Smith and Sbar, 1974, Christiansen and McKee, 1978, Stickney and Bartholomew, 1987, Alt et al., 1988, Hamilton, 1989). Recent seismogenic activity of this region includes the 1959 **M7.5** Hebgen Lake earthquake on the Madison fault, the 1983 **M7.3** Borah Peak earthquake on the Lost River fault, and a 1999 **M5.3** earthquake in the Red Rock valley. A relationship between the hot spot and fault activity in its wake is predicated on a demonstrable change in fault kinematics and rupture history as a function of proximity.

Located in southwest Montana, the Red Rock fault provides an opportunity to demonstrate these changes in kinematics and rupture history using a diverse suite of geomorphic and structural data. A range-front normal fault, the Red Rock fault exhibits prominent fault scarps and significant along strike morphologic variation trending tens of kilometers across several fault segments. Previous studies have suggested two segments along the Red Rock fault, although these studies disagree on the placement of the segment boundary (Haller, 1988, Greenwell, 1997). As fault rupture length is related to earthquake magnitude (Wells and Coppersmith, 1994), studying segmentation has received particular interest. A fault segment may possess and be delineated by a unique set of one or more physical properties such as characteristic seismicity, rupture frequency, strike orientation, scarp morphology, footwall topography, and hanging wall fan geometry (e.g. Dodge and Grose, 1980, Schwartz et al., 1982, DePolo et al., 1991, Turko and Knuepfer, 1991, Wheeler, 1987, McCalpin, 1996). Ultimately, segmentation reflects the characteristic rupture behavior of a fault. The various methods utilized to identify segments are in fact describing segmentation, and thus fault rupture history, over a range of recording windows. As surficial features are influenced by a number of mechanisms in addition to tectonics including lithologic and climatic factors, an iterative comparison of the various segmentation records is required to isolate and quantify real tectonic signals in the context of these other influences. Numerous studies in the Yellowstone/Snake River Plain area have not synthesized segment rupture histories into a single model for long term tectonic deformation associated with the hot spot. This study aims to provide such a synthesis as well as

refined criteria for defining segments based on geomorphic principles that account for the relative sensitivity of the uplifted footwall, river channels, and hanging wall fans to tectonic deformation.

This study provides constraints derived from a comprehensive consideration of geomorphic and geochronologic data extracted from the hanging wall, footwall, and fault zone in order to define segmentation along the Red Rock fault over a range of time scales. Numeric radiocarbon ages are used to calibrate relative soil development of several fan and terrace surfaces proximal to the fault. These dated deposits provide the main criteria for documenting the location and frequency of segment rupture along the entire strike length of the fault. The planimetric distribution of these dated alluvial fan units preserve a record of the relative magnitude and distribution of accommodation space in the down-dropped hanging wall (e.g Bull, 1961, Denny, 1967). A series of channel and drainage basin metrics extracted from footwall drainages record fluvial response to offset at the range front. With an established knowledge of the record lengths inherent to the various geomorphic indices, synthesis of the entire data set permits the assembly of a record of segmentation along the Red Rock fault over a range of time scales, and the extrapolation of a tectonic history. A history of segmentation is instructive into the kinematics of rupture distribution along the Red Rock fault and helps to constrain regional tectonics in the northern arm of the Yellowstone hot spot wake.

GEOLOGIC SETTING

The northwest-southeast trending Red Rock fault is an east dipping range front normal fault along the eastern side of the Tendoy Mountains, in southwestern

Montana (Fig 2). Regionally, the Laramide Blacktail-Snowcrest uplift exposes mid-crustal rocks 20 km to the northeast of the Red Rock fault, in the Blacktail Range. To the southeast and north (respectively), are the active north dipping Centennial and west dipping Monument Hill normal faults. Farther to the west are the Beaverhead, Lemhi, and Lost River Ranges (respectively). Each of these ranges are cored by Paleozoic or older sedimentary and metasedimentary rocks, and are bound on their western flanks by an active range front normal fault. While these faults are similar to the Red Rock fault in that they exhibit similar strike orientation and normal displacements, the Beaverhead, Lemhi, and Lost River Faults are dissimilar from the Red Rock fault in a number of significant ways. These faults all dip to the west, are 3 to 4 times the strike length of the Red Rock fault, have topographically higher footwalls, and have no transverse drainages. First noticed by Virgil Kirkham in 1927 (Anders, 1997), these faults also possess hanging wall basins with divides that drain both to the north (into the Salmon River Basin) and south into the Snake River basin. Comparatively, the Red Rock and Centennial Valleys are drained by the Red Rock River, which flows to the north and east into the Missouri River catchment.

Obvious scarps along the eastern base of the Tendoy Range begin just south of the mouth of Little Sheep Creek and trend north discontinuously until they become obscured near McKnight Canyon, a total strike length of ~20 km. The scarps offset Quaternary alluvial fans and terraces. From Little Sheep Creek to Chute Canyon the fault shows dramatic topographic expression, with multiple scarps and prominent footwall faceted spurs that rise abruptly above the Red Rock Valley. North of McKnight

canyon, although lacking definitive scarps in late-Quaternary units, the fault can be traced until just north of Limekiln Canyon, extending the total strike length to ~28 km.

Along its strike length, the fault offsets variable lithologies and Sevier thrust related structures within the footwall range (Scholten et al., 1955, Klecker, 1980, Lonk et al., 2000). In the south and central portions of the footwall, from Little Sheep Creek to Big Sheep Creek, the fault offsets extensive deposits of syn-orogenic conglomerates of the Late Cretaceous Beaverhead Group (Williams, 1984, McDowell, 1989). Further hinterward (to the west), Paleozoic carbonate and clastic units in the Tendoy and Four Eyes Canyon thrust sheets of the Sevier thrust belt underlie the higher peaks of the Tendoy Mountains. A small salient in the front of the Tendoy thrust sheet in the vicinity of Little Water Canyon results in the Red Rock fault locally offsetting Paleozoic and lower Mesozoic units. Here, a steeply hinterward plunging, kilometer-scale anticline-syncline pair exists at the range front. Further north, the Tendoy thrust arcs back to the west, leaving the Red Rock fault to again offset Beaverhead Group strata before eventually dying out in Mississippian units near its northern terminus. The Tendoy thrust represents the most eastward exposed thrust sheet of the Sevier fold and thrust belt in this area (Bartholomew, 1989).

A sharp topographic contrast exists between the hanging wall and footwall of the Red Rock fault. The hanging wall is capped with fan gravels generated in the Tendoy Mountains and generally slopes gently eastward away from the range to the Red Rock River. Red Rock Butte, near the town of Dell, is a 3-4 km wide mesa composed entirely of Beaverhead conglomerate, providing a glimpse into the otherwise buried Cretaceous

geology of the hanging wall. Further east, bedding within extrusive and sedimentary units of the Tertiary/Neogene Sixmile Creek Formation and the Timber Hill basalt slope gently to the southwest (Fields et al., 1985). In the footwall of the Red Rock Fault, the Tendoy Mountains rise above the Red Rock valley with a maximum relief of 1.1 km (at Dixon Mountain). The range is deeply incised as Big and Little Sheep Creeks traverse the 8-12 km wide range to head in areas west of the Tendoy. The footwall between the transverse streams is incised by a number of small drainage basins with ephemeral streams.

Hanging wall alluvial fans are offset by the fault at their heads across several of the drainages. These fans are composed predominantly of three allostratigraphic units whose sedimentology and morphology are distinct, found at many locations along strike, and are correlative between locations. Obvious scarps also offset river terraces that are genetically related to the fan deposits in both Little and Big Sheep creeks. For example, a 3 meter scarp in the fans and terraces at Big Sheep Creek also expressed by a knick-zone in the channel ~25 meters upstream from the fault. A 2-meter scarp at Little Sheep Creek is documented along side at least one additional set of uplifted terraces in the proximal footwall (Johnson, 1981, Haller, 1988).

Previous Work

Trenching, fault scarp morphology, and fan metrics have been completed to qualitatively and quantitatively describe the distribution and displacement histories of segments along the Red Rock fault. A trench dug across the fault scarp at the mouth of Little Sheep Creek yielded evidence of two offsets over the last 10 ka. to 15 ka.

(Stickney et al., 1987)(Fig. 2). The younger offset was dated at 3 ka. +/- 800 years and a minimum age on the older offset was estimated to be ~9 ka.

Two segments have been proposed on the basis of scarp morphologies, with a segment break just north of Big Sheep Creek (Johnson, 1981, Haller, 1988, Crone and Haller, 1991)(Fig. 2). A few locations south of Garr Canyon exhibit multiple scarp traces. These scarps are interpreted to represent at least two discrete offset events separated by 5,000 to 7,000 years. North of the proposed segment break, scarps are generally shorter, less steep, and discontinuous.

Planimetric aspect ratio and slope quantitatively describe the three-dimensional shape of hanging wall fans. Significant variation in fan morphology along strike of the Red Rock fault also suggests two segments, with a segment break near Little Water Canyon, north of that determined by the scarp data set (Greenwell, 1997). Small steep fans in the south are interpreted to represent the accommodation space afforded by greater amounts of recent offset along this segment. Comparatively, broad gentle fans in the north indicate less accommodation space due to less offset.

METHODS

Proximal hanging wall fans, their footwall fan heads, and visible fault scarps were mapped from 1:30,000 scale vertical aerial photos and field work. Multiple fan units were observable in many locations. We have proceeded on the assumption that episodic deposition of fan units is likely a result of varied sediment supply, attributed primarily to climatic change and to a lesser degree tectonically driven local base level fall (e.g. Lustig, 1965, Ritter et al., 1993). At least four fan units (Qf1 through Qf4)

mapped on the basis of sedimentology, stratigraphy, surficial morphology, and a crude, field-based soil chronosequence. Soil pits dug into proximal footwall fan surfaces at the mouths of drainages provided material for both absolute and relative dating of fan depositional ages. Soil profiles were described down to a depth of at least 1 meter and detrital charcoal was collected for ^{14}C analysis. In the absence of datable material, relative soil development provided age constraints as well, as a basis on which to correlate fan deposits along the range front.

Soils in a semi-arid climate like that in the American west accumulate pedogenic carbonate over time. The degree of this pedogenic carbonate development generally increases with the age of a soil, but is also strongly influenced by other factors including parent material, aerosolic dust content, and local root respiration rates. Field morphologic description of pedogenic carbonate can be used as a crude measure of relative soil age (e.g. Gile et al., 1966, Birkeland, 1999). Clast counts were conducted at pit sites to determine the relative percentage of carbonate in the parent material.

A number of previous studies calibrated carbonate stage development of western soils to absolute soil ages determined from ^{14}C analysis of detrital charcoal (e.g. Reheis, 1987, Ritter et al., 1993). Local wildfires are likely every few centuries in semi-arid climates, as such, fluvial and debris flow deposits commonly contain appreciable amounts of detrital charcoal (Pierce and Meyer, 2001). Five ^{14}C dates and eight soil pits constrain the age and correlation of the fan deposits.

Observed offset in the various fan units provides boundary ages for the most recent surface rupture along strike. Map patterns in the multiple hanging wall fan units

are also a crude measure of recent tectonism. Channelized fan units imply entrenchment of those units into older materials. Comparatively, large surface area, broad, lobate exposures indicate blanketing deposition of younger fan units over older materials. Fans dominated by blanketing deposition of subsequent units imply an ongoing generation or surplus of accommodation space. Topographic analyses of the footwall range were conducted to ascertain the persistence of rupture patterns in the longer-term uplift history of the range. Specifically, the geometries of 21 ephemeral drainage basins emptying eastward into the Red Rock Valley were quantitatively described using slope long profiles, length gradient indices, basin hypsometries, volume/area ratios, basin shapes, and slope asymmetries (Table I). These parameters record longer-term landscape processes and preserve an integrated record of fault offset over a range of time scales. This provides an additional fault activity proxy with which to compare this study's rupture data set and preexisting geomorphic data sets. These analyses were limited to drainage basins of similar areas (1-5 km²) and orders (2-3), contained within watersheds underlain by the Beaverhead Group. Additionally, several basins not hydrologically connected to the fault but also underlain by Beaverhead Group lithologies were analyzed as controls. Electronic digital elevation models (DEMs), available from the USGS at 30 meter resolution, provide a reliable large scale topographic data set for this range of analysis (e.g. Franklin, 1987). Channel profiles were extracted from the DEMS starting at the mapped fault trace and extending upstream. These profiles were smoothed over a 3 to 5 data point linear window and normalized to their elevations at the fault trace for visual, qualitative comparison. Length-gradient (*SL*) indices

normalize channel slope to basin size, providing a means to quantitatively compare channel slope between basins. Length gradient indices were calculated using a 300 meter aperture window in order to resolve small (<0.5 km) deviations in channel slope.

Basin hypsometry and volume-area ratios (V/A) describe the three-dimensional shape of a basin, providing a sense of the relative degree of channel incision over an entire watershed. Basin hypsometry quantifies the elevational distribution of surface area in a particular basin. Hypsometric curves are calculated based on total basin area and total elevation gradient, and are thus normalized and comparable between basins. Hypsometric integrals quantify basin area-elevation distribution, small values are indicative of large basin areas at lower elevations and large values indicate a predominance of basin area at higher elevations. V/A ratios reflect the average depth of a basin relative to basin surface area. V/A ratios are derived from topographic data sets by comparing calculated basin volume beneath an upper enveloping surface (pinned to the drainage divides) and basin planimetric area.

Drainage basin elongation and asymmetry describe only the planimetric shape of a watershed. In this sense these metrics quantify only the areal geometry of a basin and, strictly speaking, are insensitive to vertical basin geometry. Elongation is quantified by comparing basin major and minor axes, measured through a geometric midpoint. Asymmetry is measured by comparing the area distributed on either side of a trunk channel. As such, significant trends in asymmetries could reflect regional tilting orthogonal to channel orientation.

RESULTS

Fan stratigraphy

Eight soil pits were dug into fan surfaces, four of which yielded significant amounts of charcoal suitable for analysis (Table 2, Fig. 3). Four fan deposits are defined along the Tendoy Range front, ranging in age from late Holocene to Pleistocene:

Qf1

Qf1 is the oldest recognized fan unit in the Red Rock fault hanging wall. Exposures of Qf1 are limited to a few isolated deposits along the northernmost extent of the Red Rock fault, at the mouth of Limekiln and Kelmbeck canyons (Fig. 3, km. 24-26). Qf1 exposures are composed of coarse to medium grain sized alluvium including rounded to sub-angular gravel, sand, and silt. Clasts are predominantly limestone with lesser amounts of rounded quartzite, exhibiting affinities to the Paleozoic and Cretaceous bedrock exposures in the Tendoy Mountains. Deposits of Qf1 are incised by stream channels filled with younger fan units (Fig. 4). Qf1 treads exhibit a very smooth surface morphology and are 5-10 meters higher than the next younger, inset fan unit. No charcoal or soil data exist for Qf1 deposits, however, their landscape position above dated late Pleistocene deposits and smooth surface morphology suggest a middle or late-middle Pleistocene age.

Qf2

Extensive Qf2 deposits blanket the Red Rock fault hanging wall north of Big Sheep Creek, with fewer exposures south of the creek. The exposures fine and coalesce down fan with a very smooth or subdued bar and swale surface morphology. Along the

northern Red Rock piedmont, valleys filled with younger fan units are inset into Qf2 exposures. Qf2 soil pits exhibit well developed, stage II+ to III, pedogenic carbonate horizons as well as evidence for buried horizons. A radiocarbon age of ~10.5 ka derived from charcoal extracted from near the top of a Qf2 soil pit at Big Sheep Creek can be regarded as a minimum age for this unit. The soil, surface morphology, and widespread extent of the deposit are similar to the Qf2 deposits of Ritter et al. (1993). These observations along with the minimum radiocarbon date indicate a late Pleistocene, probably last glacial maximum, to latest Pleistocene age (~20-10 ka.) for its deposition.

Qf3

Surface exposures of Qf3 are broad and extensive adjacent to the southern Red Rock fault (Fig. 3, km. 0-10) but are confined to valleys inset into Qf2 surfaces further north (Figs. 3 & 4). Qf3 exhibits a subdued but clearly identifiable bar and swale surface morphology. Clast composition is also similar to the older Qf2 unit. Qf3 soil pits exhibit stage I+ to II pedogenic carbonate development. Charcoal collected from near the top of Qf3 deposits at two separate soil pit sites yielded radiocarbon ages ranging from 4.6 to 3.2 ka. A soil pit at Dry Canyon yielded material from two distinct horizons with the younger ages residing in the stratigraphically younger position. Qf3 was deposited in the middle Holocene, between ~5 and 3 ka.

Qf4

Qf4 deposits occur along the entire Red Rock piedmont, but are restricted in volumes and aerial extent relative to the larger Qf2 and Qf3 deposits. North of Big Sheep Creek Qf4 deposits are confined to channels inset into the older fan units. In the

south, Qf4 deposits bury Qf3 fan exposures in the Red Rock hanging wall, and are inset into Qf3 treads in the adjacent footwall (Fig. 4). Qf4 deposits exhibit a pronounced bar and swale morphology as well as modern, active channel beds. Qf4 deposits have a similar clast composition to the older fan units but are typically finer grained, dominated by sand and silt. There is little to no pedogenic carbonate development in Qf4 deposits; all soil pits exhibited stage I or less calcic horizons. A single radiocarbon age of 1.3 ka. extracted from a depth of .75 meters below a Qf4 surface indicates a late Holocene age of this unit.

Constraints on fault segmentation

Fan unit distribution

From stations 0-8 on fig. 3, from Little Sheep Creek to Garr Canyon, exposures of Qf3 and Qf4 surfaces dominate, whereas Qf2 exposures are observed only in the Chute and Garr canyon fan systems (figs. 3 & 4). Qf3 and Qf4 surfaces are not significantly entrenched anywhere in the fan system. Further north, from north of Garr Canyon to Dry Canyon (Fig. 3, km. 9-17), Qf2, Qf3, and Qf4 units are all present on the surface, although the total percentage of fan surface covered by Qf3 and Qf4 units is reduced when compared to the south. Also, the Qf4 and Qf3 deposits are progressively more entrenched into the Qf2 deposits (Fig. 4). North of Dry Canyon (Fig. 3, km. 17-27) the hanging wall is dominated by Qf2 exposures and isolated exposures of Qf1 are present. Both Qf3 and Qf4 deposits are deeply entrenched within the older fan units.

Scarp distribution

Prominent scarps along the range front offset Qf2 and Qf3 surfaces nearly continuously from just south of Little Sheep Creek to ~0.5 km north of Chute canyon (Fig. 3, km. 0-7), where scarps are obscured by a landslide. Qf4 surfaces are not faulted along this strike length. At Garr Canyon, the range front steps ~0.5 km eastward and no scarps are present within any fan unit. Scarps appear again ~0.5 km north of Garr Canyon. These scarps extend discontinuously north until ~1 km north of Little Water Canyon (Fig. 3, km. 9-19) and have lower relief than those observed in the south. Prominent at the mouths of Big Sheep Creek, Dry Canyon, and several other unnamed drainages, these scarps offset Qf2 surfaces but leave both Qf4 and Qf3 unfaulted. Along the northern strike length of the fault, from south of McKnight Canyon to where the fault dies out north of Limekiln Creek (Fig. 3, km. 20-27), scarps within Qf2-Qf4 are not apparent and the range front steps ~0.5 km to the east. One Qf1 deposit, however, appears to be faulted.

Footwall geomorphic indices

From Little Sheep Creek to Garr Canyon (Fig. 3, km. 0-8) footwall drainage basin channel long profiles display a prominent break in slope near the channel mouth, where gentle upper channel slopes abruptly steepen downstream towards the range front (Fig. 5). These convexities in the long profiles are evident in the length-gradient (*SL*) indices calculated along these channels (Fig. 6). *SL* values are high near stream mouths (400-600 meters), indicating steeper relative slopes, and decrease up stream (leveling out at 200-300 meters) in many of the southern drainages. The upper channel values are

equivalent to those observed in the nearby control basins, suggesting that these values reflect characteristic channel slopes within Beaverhead lithologies. Long profiles from Garr Canyon to Big Sheep Creek (Fig. 3, km. 8-12) are not distinctive from those observed further north along strike. *SL* values are consistently low from Garr Canyon to Big Sheep Creek (150-300 meters) and consistently high north of Big Sheep Creek to the northern extreme of the Red Rock fault (300-600 meters). Although the *SL* values north of Big Sheep Creek are relatively high, these indices are unperturbed proximal to the range front.

Hypsometric integrals collected from drainages south of Garr Canyon are larger relative to the rest of the data set, indicating more basin areas still standing at high elevations. Hypsometric integrals display a subtle trend of decreasing values to the north (Fig. 7), consistent with drainages where more of the basin area has been lowered closer to base level. Two basins at the northern extreme of the fault, Kelmbeck Creek and Limekiln Creek (Fig. 3, km. 24-25), do exhibit anomalously large integral values relative to the overall trend of the data set.

V/A ratio values for basins south of Garr canyon are distinctive from others along strike (Fig. 3, km. 0-8)(Fig. 8). A Mann-Whitney test of significance indicates that this population of basins have *V/A* values that are distinguishably higher than the rest of the analyzed basins (at $\alpha=0.05$) (Davis 1986). *V/A* values of basins north of Garr Canyon are consistently lower than those observed in the south, and are not distinguishable from values obtained from the control basins at the same level of significance. Higher *V/A* values reflect deeper, more incised basins.

Area/elongation values and basin asymmetries do not display the persistent along strike variability trends observed in the other morphometric indices (Fig. 8). Other patterns are, however, observable in both the basin asymmetries and elongations. Of 21 basin asymmetries analyzed along strike, 13 display greater areas to the north of trunk channels.

DISCUSSION

Segmentation along the Red Rock fault

As segmentation likely arises as a result of the unique rupture characteristics of individual strike lengths of a fault zone, segments defined by surface rupture distribution represent a direct link between observable surficial features and recent fault motion. The last three rupture events delineate three segments along the Red Rock fault. As indicated by the trenching study (Stickney and Bartholomew, 1987) and confirmed by this analysis, the southern segment last ruptured around 3 ka. This segment, defined by the 3 ka event, extends ~8 km from Little Sheep Creek to Garr Canyon (Fig. 3, km. 0-8). The central segment, defined by a last rupture age between 10 ka. and 3 ka., extends from Garr Canyon to ~1 km north of Little Water Canyon (Fig. 3, km. 8-19). This event or events likely ruptured portions of the southern segment as well, as indicated by an older rupture resolved in the Little Sheep Creek trench and multiple southern scarps. Some offset in the central segment at Big Sheep creek from the 3 ka event also seems likely. The northern segment, extending from ~1km north of Little Water Canyon until the fault is lost in the bedrock just north of Limekiln Canyon (Fig. 3, km. 19-27), is defined by a lack of recent offset, with the last rupture event occurring sometime

significantly before 10 ka. This three-segment model provides a hypothesis that can be compared to the segmentation defined by other criteria. To facilitate this comparison, surface rupture is used heretofore to define the south, central, and northern fault segments.

At least two significant offset events within the last 10,000 years (with more than 3 meters of offset at Chute Canyon since 4.5 ka.) are indicative of the active tectonism that defines the southern segment. Recent and rapid down dropping of the hanging wall Red Rock Valley exerts a strong control on channel metrics and fan geometries proximal to the fault trace. This has served to both create accommodation space for the steep, vertically aggrading fans along this segment, and to produce the base level fall which generates the deeply entrenched, steep channel extents proximal the range front. This pattern is especially apparent where channel convexities and high *SL* values proximal to the fault trace tightly constrain the southern segment.

The central segment has experienced less overall activity in the last 10 ka., with only one definitely resolvable surface rupture over that time period. A lack of observable channel response to tectonism and lower *V/A* ratios in this segment when compared to the south implies persistent diminished faulting activity. The *SL* values recorded in the basins north of Big Sheep Creek are likely a result of either more resistant bedrock characteristics or a different landscape response to tectonic influence than observed in the south, as the divides of these basins are held up by resistant units in the Tendoy thrust sheet and the channels show no perturbation proximal to the fault. Fan distributions and metrics, when reexamined with a segment break at Garr Canyon, do

display a subtle variation between the central and southern segments. The lack of any scarp expression at Garr Canyon accompanied by a lateral step in the mountain front strengthens the interpretation of a segment boundary at this location. A break in surface rupture accompanying a lateral step in an active range front is a commonly observed feature frequently used to define segment boundaries elsewhere (e.g. Crone et al. and Haller, 1991, Zhang et al., 1991).

The boundary between the central and northern segments is clearly resolvable in the loss of scarp expression north of Little Water Canyon and a significant change in fan metrics between Dry and Little Water Canyons (Greenwell, 1997). Basin metrics, despite failure to distinguish this segment boundary, agree with fan metrics and surface rupture records by indicating the lack of a strong tectonic signal along the northern segment. Observable fault offsets disappear in Paleozoic bedrock at the northern limit of this segment, implying that total throw along the northern segment of the Red Rock fault is small.

The 1999, M5.3 event in the vicinity of Kidd was not projected to have occurred along the Red Rock fault plane, although the focal mechanism suggests offset along a blind conjugate fault near the northern tip of the Red Rock fault (Stickney and Lageson, 2002). While this event was not accompanied by any surface rupture, it still serves to highlight the ongoing seismicity of the Red Rock Valley. The 1999 event also holds implications for the characteristics of rupture and seismicity along the Red Rock fault. The lack of any surface rupture implies that either a larger magnitude or shallower focus event is required to generate the surface ruptures presently visible along the fault. This

brings into question the accuracy of paleoseismic reconstructions assembled from surface rupture data.

Record-length characteristics of tectonic indices

The varied indications of segmentation and tectonism returned by the suite of fault plane, hanging wall, and footwall data sets is instructive into both the kinematic history of the Red Rock fault and the response dynamics of drainage basins and fan systems to fault activity. Surface rupture distribution, scarp morphology, fan metrics, fan distribution, channel gradients, and basin *V/A*s indicate an increase in tectonism in the south, especially in the southern segment. Channel metrics and basin *V/A* record the southern segment break at Garr Canyon, but not the northern break between the north and central segments. Fan metric and fan distribution data roughly agree with the placement of this northern break, but do not indicate the southern segment break. Basin hypsometries display a subtle along strike trend consistent with increased tectonism in the south, but fail to clearly distinguish segments. The two anomalously high hypsometric values from the northern extreme of the fault are likely the result of lithologic factors, as the upper portions of these drainage basins are underlain by Paleozoic units (Fig. 2). Elongation and asymmetry fail to show any convincing along strike trend and thus do not preserve a record of segmentation. Along strike distribution of recorded small magnitude seismicity in the Red Rock valley suggests segmentation, although events are predominantly clustered adjacent to the northern segment (Stickney and Lageson 2002).

Footwall indices that are sensitive to the three-dimensional geometry of a basin are capable of resolving the relatively short-term tectonic events along the Red Rock fault. The ability resolve shorter term tectonic signals comes about because these fluvial systems are responding to a base level drop first through incision. This is apparent in the steeper channel profiles proximal to the south range front. V/A and hypsometry records show this relationship in a more subtle fashion because these indices integrate morphometric data over an entire basin. As a result, the deeper valleys along the more incised lower reaches of channels are evident, but muted by the effects recorded over the rest of the basin. Comparatively, basin area metrics, like elongation and asymmetry, do not record the observed activity gradient. These metrics are either insensitive to Red Rock fault tectonism, or more likely, require significantly longer times to respond to base level fall. This suggests that the processes that effect basin area distribution, such as drainage capture and lateral channel erosion, operate over longer time intervals. The current segmentation behavior along Red Rock fault has potentially not been active long enough for basin area metrics respond. However, the slightly elongate and asymmetric characteristics of these basins may represent a subtle tectonic signal. Of particular interest is the general pattern of greater area on the north sides of basins, potentially the result of down the south regional tilting associated with subsidence of the Snake River Plain (e.g. Cox, 1994).

Utilizing the known ages of fan surfaces, coarse estimates on the response times and integrated record lengths of the various tectonic indices can be made (Fig. 9). Seismicity and surface rupture record tectonism instantaneously whereas fan distribution

and fan metrics operate and preserve records over the thousands to hundreds of thousands of years required for fan development. Three-dimensional channel metrics respond at the same time scales as fans, but may require a greater amount of total fault offset (and thus time) to develop a strong tectonic signature. The inability to resolve a tectonic signal recorded by adjacent fan systems implies that basin area indices require even longer response times. Basin area indices, in turn, likely record a tectonic signal convolved over the longest time spans, relative to the rest of the data set.

Red Rock fault kinematics and dynamics

Longer term, integrated records of tectonism such as three-dimensional basin metrics broadly agree with short-term records in elucidating an along strike gradient in tectonism along the Red Rock fault. This implies that the recent activity gradient is representative of the longer-term kinematic behavior of the fault. The lack of throw along the northern segment suggests that this behavior has persisted throughout the entire life of the fault. It is likely that the majority of mountain front relief along the Red Rock fault is inherited from exhumed Sevier thrust belt structures rather than as a direct manifestation of footwall displacement. The greatest mountain-front relief is along the northern central and northern segments, above a structural culmination in the Tendoy thrust sheet.

The displacement gradient along the Red Rock fault resembles a tear. Maximum total offset in the southern segment gradually diminishes northward. The rupture that offsets Qf2 is observable in both the south and central segments whereas the rupture that offsets Qf3 is definitively observable only in the south. This suggests that the offset

gradient is due to the combination of more frequent events confined mostly to the south segment, less frequent events over both segments, and rare events that rupture along the entire fault. The discordance between tectonic records preserved by basin area metrics and the other indices implies that the current activity gradient along the fault has been operative only recently, over time spans shorter than those integrated by basin area metrics. That basin area metrics fail to record a strong tectonic signal indicates either that the observed characteristic fault activity was initiated only recently (over these same time spans) or that the fault has not been active in way that is recordable by these metrics.

Offset Neogene volcanic flows and sediments within the Sixmile Creek Fm. constrain the initiation of Tendoy Mountain uplift, and thus Red Rock fault activity, at ~6-5.5 Ma (Fritz and Sears, 1993). To the west, the Lost River, Lemhi, and Beaverhead faults are much longer with strike lengths of 40 to 60 km, compared to 27 on the Red Rock fault, and exhibit much greater throws. Whereas the Red Rock fault probably has a maximum offset of less than 1 km (constrained via shallow (4°-6°) southwestward dips in the 6 Ma. Timber Hill basalt) (Hurlow, 1995), the Lost River fault exhibits multiple kilometers of offset (Stein and Barrientos, 1985). As compared to the more westward range front normal faults north of the Snake River Plain, the Red Rock fault appears to be the youngest.

The apparent youth of the Red Rock fault defines an eastward younging of range front normal faults north of the Snake River Plain, which tracks the development of the topographic swell and deformation in the wake of the Yellowstone hot spot. This spatial

and temporal relationship supports the genetic link between these faults and the lithospheric flexure that exists along the flanks of the Snake River Plain (McQuarrie and Rodgers, 1998)(Fig. 10). This flexure has developed between the subsiding Snake River Plain and the adjacent uplifted hot spot wake, and likely plays a role in the variable along strike offset history of the Red Rock fault. Parallelism of the Sevier structural grain and normal fault orientation suggest structural control. Given the age and position of past eruptive centers, the hotspot would have first been at a position to influence Red Rock Fault activity around 6 Ma., a number confirmed by the offset volcanic flows and sediments proximal to the Tendoy Mountains. It would be difficult to argue that northern Basin and Range crustal extension is due solely to hot spot activity, given that regional tension exists all along the Cordillera and especially to the south in the Basin and Range province (Zoback and Zoback, 1989). In the northern Rocky Mountains, however, total crustal extension is greatest near the Snake River Plain and rapidly decays north of the hot spot wake. This implies that the potential for crustal extension is ubiquitous north of the Snake River Plain, but this extension is exacerbated within this region due to a local stress field produced by lithospheric flexure within the hot spot wake.

Influence of faulting and hotspot on regional drainage

In the interest of assembling a comprehensive understanding of the regional structural and landscape evolution associated with the hot spot, it's useful to consider the potential future development of the Red Rock fault. If this fault were to evolve similarly

to the other range front faults north of the Snake River Plain, then continued rupture will eventually extend the fault length southward across the Lima peaks, or link up with smaller faults recognized to the southeast, in Monida pass (Fig. 10). Continued offset would accommodate the headward (northward) migration of Snake River drainage divide, allowing the eventual capture of the headwaters of the Red Rock River and resulting in a low drainage divide somewhere in the Red Rock valley, similar to the drainage divides in the Beaverhead, Pasemeroi, and Lost River Valleys to the west. With the continued northward migration of the Snake River drainage divide, the headwaters of Big Sheep Creek might be diverted to the south, instead of east through the Tendoy Mountains, leaving a new divide along the old Big Sheep Creek channel and a deeply incised pass in the range, similar to Double Springs Pass and Pass Creek in the Lost River Range. Considered together, these features allow for an evolutionary sequence of fault development in the northern Basin and Range. This time-transgressive fault development parallels the relative northeastward migration of the Yellowstone hot spot.

CONCLUSIONS

The Red Rock fault exhibits variable displacement along strike. Based on the distribution of dated rupture events, three segments are resolvable along the fault, with a segment break similar to that previously suggested near Little Water Canyon, and a previously unidentified break at Garr Canyon. Multiple Holocene rupture events are evidence of rapid, ongoing hanging wall down-drop along the southern segment. The

central and northern segments exhibit progressively lesser amounts of both recent and total offset. The northern segment has not experienced significant surface rupture since at least the late Pleistocene and total displacement along the fault here is small.

The diverse range of topographic and geologic features commonly used to delineate fault segmentation are responding to, and preserving a record of fault offset over diverse temporal and spatial scales. It follows that the metrics used to quantify these morphologies are defining segmentation over a range of time scales and number of rupture events. A coarse quantification of these inherent time scale lengths is made by comparison of segmentation records preserved by dated landforms (alluvial fan units) and landforms that are more difficult to age characterize (drainage basin morphologies). This serves to highlight the progression of landscape response to fault offset and permits the assembly of a long-term fault kinematic history. The concordance of segmentation records preserved in alluvial fans and channel profiles imply that fluvial systems have the ability to rapidly respond base level fall due to hanging wall offset initially through channel incision, followed later by slower processes that affect planimetric basin areas.

The long-term record of fault offset preserved in some footwall drainage basin metrics indicates that the distribution of Holocene and Late Pleistocene activity recorded by surface ruptures reflects the long-term behavioral characteristics of the fault, over time periods likely extending to earlier in the Pleistocene and Pre-Pleistocene. Geologic evidence constrains the earliest activity of the Red Rock fault to after 6-5.5 Ma (Fritz and Sears, 1993). Within the planimetric basin area indices, the lack of a distinguishable tectonic signal suggests that either the fault has recently become more

active or experienced a significant shift in characteristic kinematics over the time interval preserved by these indices. Given the apparent youth of the Red Rock fault, this structure became active much more recently than other more western range front faults north of the Snake River Plain, defining an eastward developmental trend of brittle deformation in the wake of the Yellowstone hotspot. The variable displacement geometry of the Red Rock fault in combination with the eastward younging and the spatial distribution of these range front faults imply a strong link between lithospheric flexure due to subsidence of the Snake River Plain and this regional deformation. Crustal tension and incipient extension of this region is likely exacerbated by the additional stress introduced by this flexure. When compared to the Lost River fault, it is possible to both suggest some conclusions about the future of the Red Rock fault and reconstruct the past evolution of the older northern Basin and Range faults. Continued offset along the Red Rock fault may eventually increase the strike length, increase mountain front topography, and promote capture of the Red Rock River headwaters by the Snake River drainage system.

TABLE I: DRAINAGE BASIN GEOMORPHIC INDICIES

Metric	Symbol	Equation	Variables	Sensitivity
Stream Length Gradient Index †	SL	$SL=(\Delta H/\Delta L) \cdot L$	L : distance from channel mouth ΔH : interval channel elevation change ΔL : interval channel distance	channel slope
Hypsometric Integral ‡	V/HA	$\frac{V}{HA} = \int x dy$	$x dy$: basin area x over elevation interval dy	basin area-altitude distribution (3-D basin shape)
Basin Volume/Area §	V/A	$V/A = V_1 / A_1$	V_1 : basin volume A_1 : basin planimetric area	normalized basin volume (3-D basin shape)
Basin Asymmetry #	AF	$AF=100 \cdot (A_r/A_t)$	A_r : area of one basin side A_t : total basin area	basin area distribution (2-D basin shape)
Basin Elongation ††	E_r	$E_r = D_l / D_s$	D_l : basin long axis length D_s : basin short axis length	basin geometry (2-D basin shape)

† Hack, 1973. ‡ Strahler, 1952; Fike and Wilson, 1971. § Frankel, 2002. # Hare & Gardner, 1985; Cox, 1994. †† Bull and McFadden, 1977.

TABLE II: FAN AND TERRACE UNIT SOIL PIT DATA

Location	Pit # †	Horizon	Depth (cm)	Carbonate stage	¹⁴ C age ‡	Fan unit	Age range
Garr	1	A	0-22	I	N/A		
		Bk	22-70				
		Bkb	70-106	II (buried soil)			
		C	106-113				
B. Sheep Creek Trib.	2	A	0-16	I	1290 +/- 40	Qft4	late Holocene (< 3 ka)
		Bk	16-52				
		C	52-200+				
Little Water	3	A	0-25	I	N/A		
		Bk	25-63				
		Cb	63-75				
		C	75-100				
Chute Canyon	4	Ac	0-24	I+ to II	4560 +/- 60 (bulk)	Qft3	middle Holocene (5-3 ka)
		Bt	24-40				
		Bk	40-65				
		Btk	65-105				
		C	105+				
Dry Canyon (lower surface)	5	A	0-16	I+ to II	3230 +/- 40 3520 +/- 40		
		Bk	16-77				
		Cbk	77-111				
		C	111-120				
B. Sheep Creek	6	Bk	0-59	II+	10480 +/- 60		
		Ck	60-110				
B. Sheep Creek	7	A	0-25	II+ to III-	N/A	Qft2	latest Pleistocene (~20-10 ka)
		Btk	25-41				
		Bk	41-90				
		Ck	90+				
Dry Canyon (upper surface)	8	A	0-13	III	N/A		
		Bk	13-62				
		Bc	62-80				
		Cb	80-110				
Kelmbach Canyon	N/A	N/A	N/A	N/A	N/A	Qft1	(late-middle to late Pleistocene)

† Fan and terrace soil pit data locations are keyed to plate 1.

‡ calibrated radiocarbon ages are displayed

FIGURE CAPTIONS

Figure 1. Map of the Yellowstone hot spot, Snake River Plain, and surrounding region, position of the seismogenic and topographic wake is shaded (Pierce and Morgan 1992, McQuarrie and Rodgers 1998). Names of some of the major active faults in the northern Basin and Range are shown along with the (1) Hebgen Lake, (2) Borah Peak, and (3) Red Rock valley earthquake epicenters. State abbreviations are given for spatial reference and the area diagrammed in figure 2 is boxed in.

Figure 2. Geologic map of the Red Rock fault. Names of some of the proximal footwall drainage basins are shown for spatial reference. A previous study utilized scarp morphologies to delineate a segment boundary (a) (Haller 1991). This boundary disagrees with that indicated by fan metrics (b) (Greenwell 1995). Locations of the trenching study (1), multiple scarps (2), and the knick point in Big Sheep Creek (3) are highlighted.

Figure 3. Map of scarps, Quaternary fan and terrace units identified along the Red Rock fault. Locations of soil pits, the trenching study (Stickney et al. 1987), and major named drainages are shown. Segment boundaries delineated by this study based the relationship of these fan and terrace units to fault ruptures. Numbers along the bottom of the figure are used for spatial reference in the text and are equal to kilometers along strike north of the southern fault terminus.

Figure 4. Maps and schematic cross-sections depicting the characteristic exposures of various fan and terrace units (A) south of Big Sheep Creek, and (B) north of Big Sheep Creek. Subsurface positioning of contacts is hypothetical.

Figure 5. Select channel long profiles extracted from footwall drainage basins distributed along strike. Channel elevations are normalized to the basin mouth altitude. The south drainages profile (solid line) is representative of the collective profiles extracted from five basins distributed from Little Sheep Creek to just south of Chute Canyon. Locations of the other profile drainages are identified on figure 4. A significant break in grade and channel convexity is observed in the lower .5 km of the south drainages.

Figure 6. Contour map of the *SL* values computed along all analyzed channels. Major named drainages are delineated and basins are outlined by their divides. In the south,

persistent values of 100-300 meters deviate to higher values proximal to the range front. Segment breaks inferred from this study are shown for reference.

Figure 7. Footwall drainage basin hypsometric integral values. An example of a hypsometric curve for a basin near the southern terminus of the fault is shown. Curve area values are plotted against basin distance along strike.

Figure 8. Basin volume and area geometries: **A.** Basin Volume/Area (V/A) ratios plotted against basin location north of Little Sheep Creek, control basin values are also included. Basin population mean values are indicated by horizontal bars. **B.** Basin area asymmetries; as trunk channels trend predominantly E-W, basin areas were calculated on the north and south sides of trunk channels. Each bar represents the larger side of a single basin. **C.** Basin elongations; these values display considerable variation along strike. Note the overall higher elongations observed along strike than in the control basins.

Figure 9. A. Conceptual plot of the relative sensitivities (ability to record small offset or magnitude events) of various active tectonic data sets, plotted against their event integration time spans. Estimated response times are in years. The indices are shaded to indicate whether the data sets sample the fault plane, hanging wall, or footwall. **B** indicates the number of segments distinguished along the Red Rock fault by each data set, as a proxy for the resolution capabilities of each index.

Figure 10 A. Shaded elevation map of the eastern Snake River Plain, Yellowstone hot spot, and surrounding region highlighting the Red Rock fault's position within this active tectonic framework, background elevation data extracted from the GTOPO30 digital data set. The Lost River (LR), Lemhi (LH), and Beaverhead (BH) faults are highlighted along with locations of physiographic features mentioned in the text. Drainage divides outline three major watersheds, the Snake (Sn), Salmon (Sa), and Missouri (Mo). **B.** Conceptual cross-section b-b' illustrates the lithospheric flexure along the northern flank of the Snake River Plain that is influencing Red Rock fault tectonism. The north-south lithospheric flexure gradient across this region may be responsible for the interpreted displacement gradient along fault.

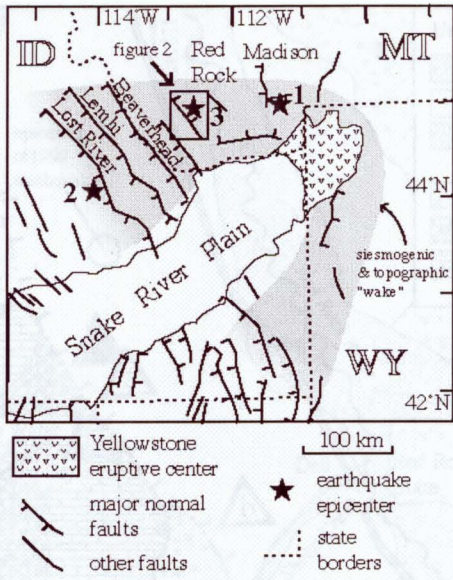


Figure 1

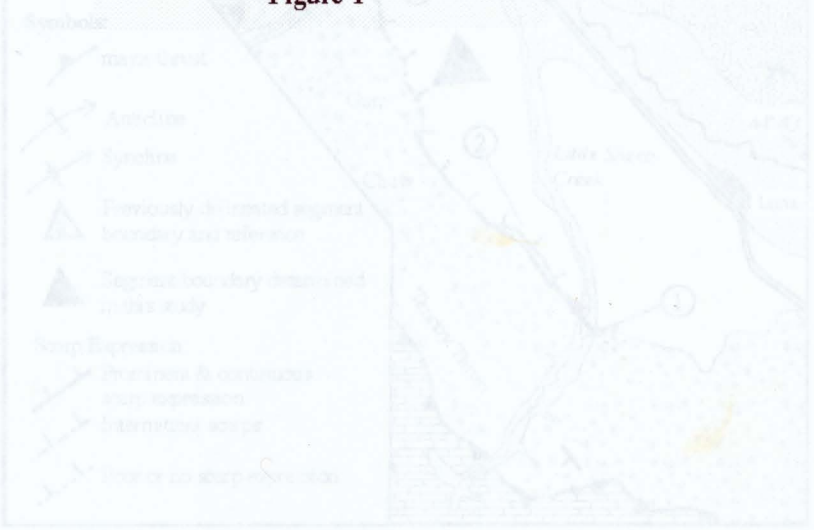


Figure 2

Figure 2. Geologic map of the Red Rock fault

Figure 1. Map of the Yellowstone hot spot

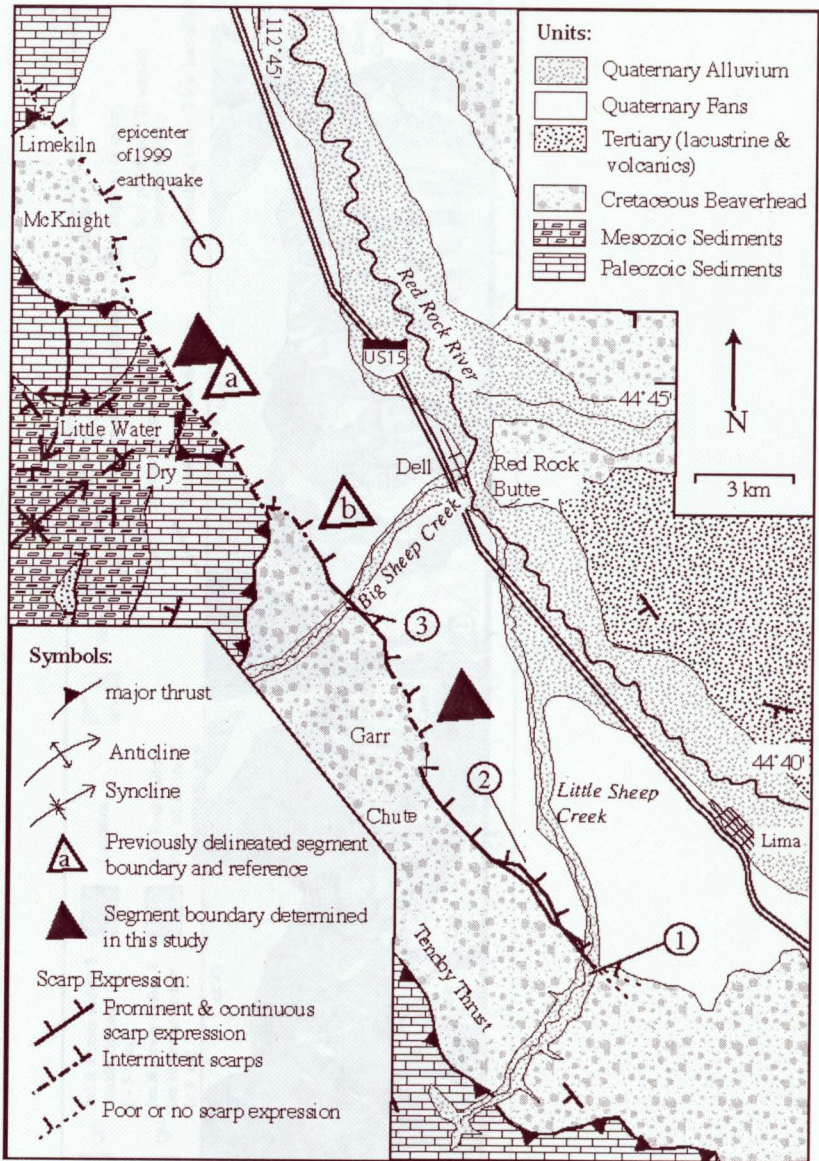


Figure 2

Figure 2. Geologic map of the Red Rock fault

Figure 3. Map of Quaternary fan and terrace fans along the Red Rock fault

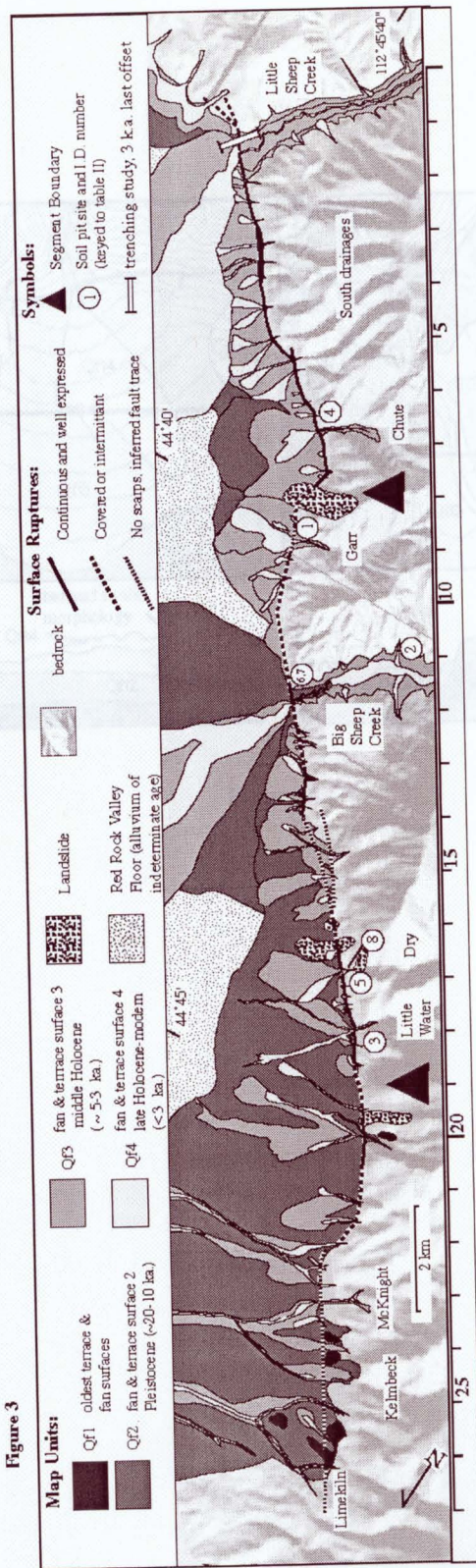


Figure 3. Map of Quaternary fan and terrace units along the Red Rock fault

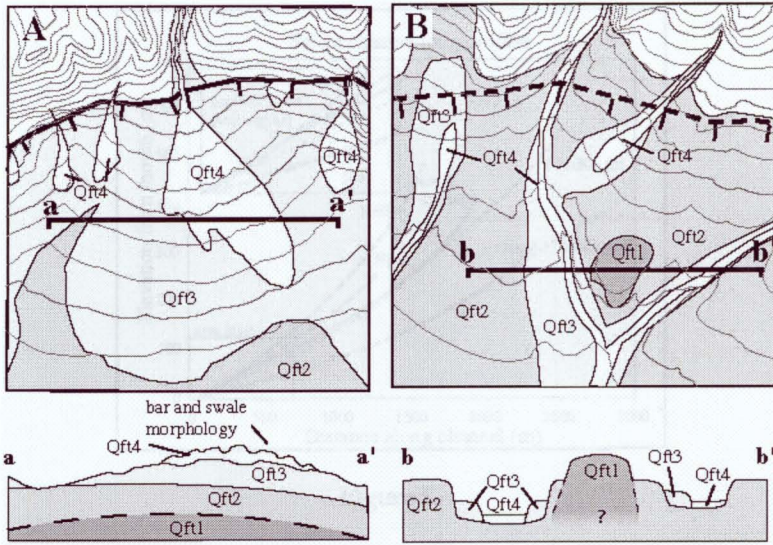


Figure 4

Figure 4. Maps and cross-sections of various fan and terrace units

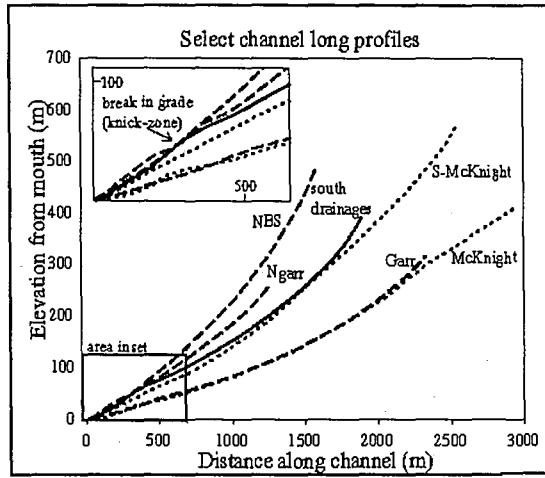


Figure 5

Figure 5. Select channel long profiles

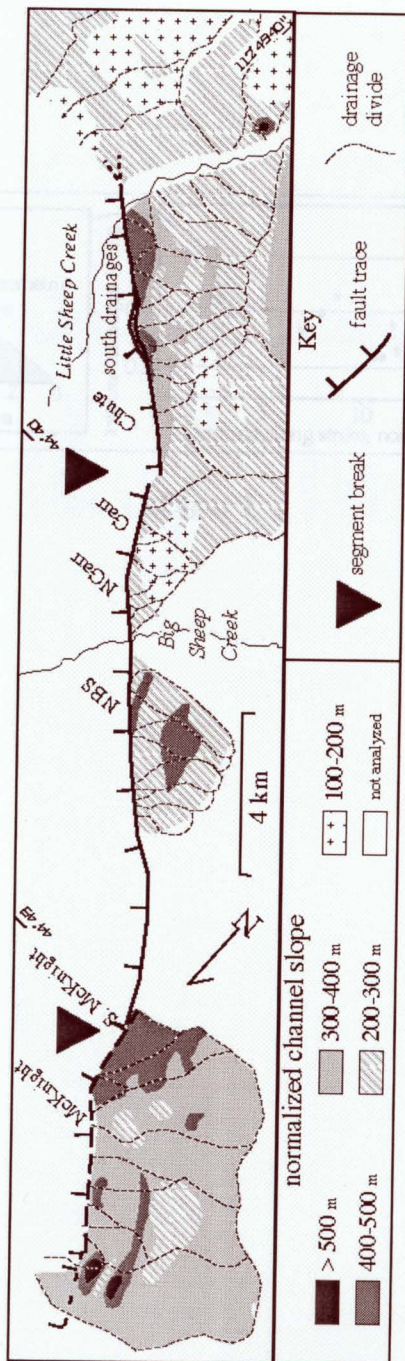


Figure 6

Figure 6. Contour map of *SL* values within footwall basins

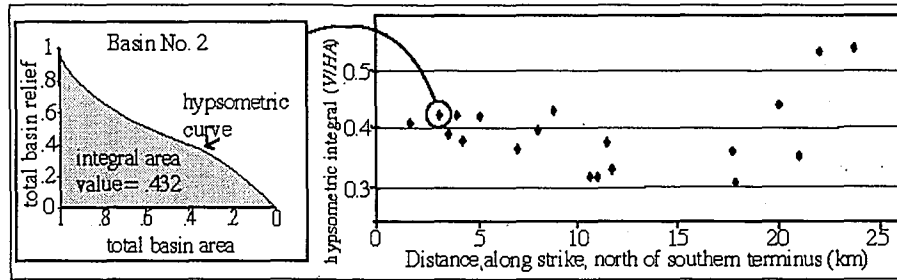


Figure 7

Figure 7. Footwall drainage basin hypsometric integral values

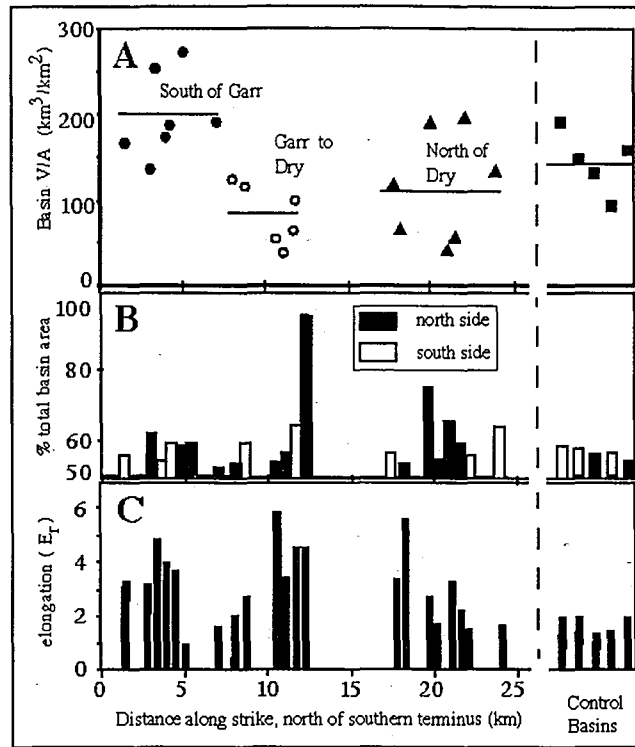


Figure 8

Figure 8. Basin volume and area geometries

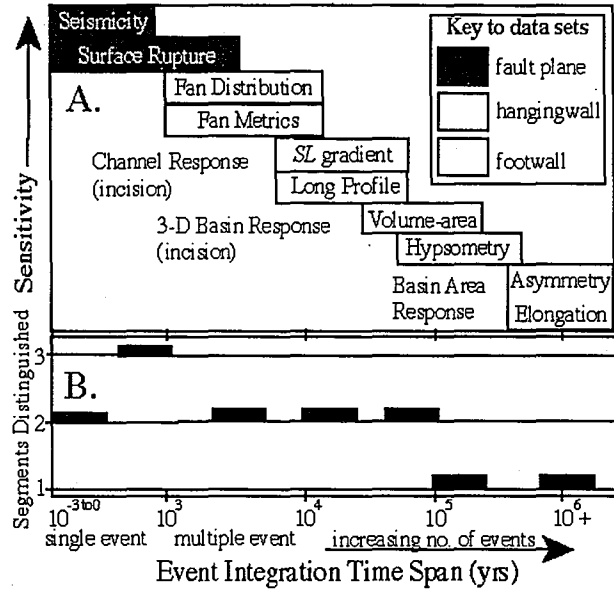


Figure 9. Conceptual plot of relative index sensitivities

REFERENCES

Alt, D., Sears, J.M., Hyndman, R.W., 1988. Tectonic evolution of the eastern Snake River Plain, p. 647-662.

Anders, M., 1961. Distribution of Quaternary faulting in the Snake River Plain, Idaho, p. 1-10.

Anderson, J.H., 1986. The Wasatch-Catchment Program: A Geomorphological Study of the Wasatch-Catchment Basin, Utah, p. 1-10.

Birkehead, Peter W., 1999. Soils and Geomorphology. New York, Oxford University Press, 430 p.

Bull, William B., 1961. Tectonic significance of radial profiles of alluvial fans in western Fresno County, California. Article 75. U.S. Geological Society Professional Paper B182-B184.

Bull, W. B. and McFadden, L.D., 1977. Tectonic geomorphology north and south of the Garlock fault, California. in Doehring, D.O., ed. Geomorphology of Arid Regions. Proceedings of the Eighth Annual Geomorphology Symposium. State University of New York at Binghamton, p. 115-138.

Christiansen, R.L., and McKee, E.H., 1979. Late Cenozoic volcanic and tectonic evolution of the Great Basin and Columbia Intermontane regions, in Smith, R.B., and Eaton, G.P., eds., Cenozoic Tectonics and Geophysics of the Western Cordillera. Boulder, Colorado, The Geological Society of America Memoir 152, p. 283-311.

Cox, Randel T., 1994. Analysis of drainage basin symmetry as a rapid technique to identify tectonic control. Quaternary Geochronology, 9, p. 571-581.

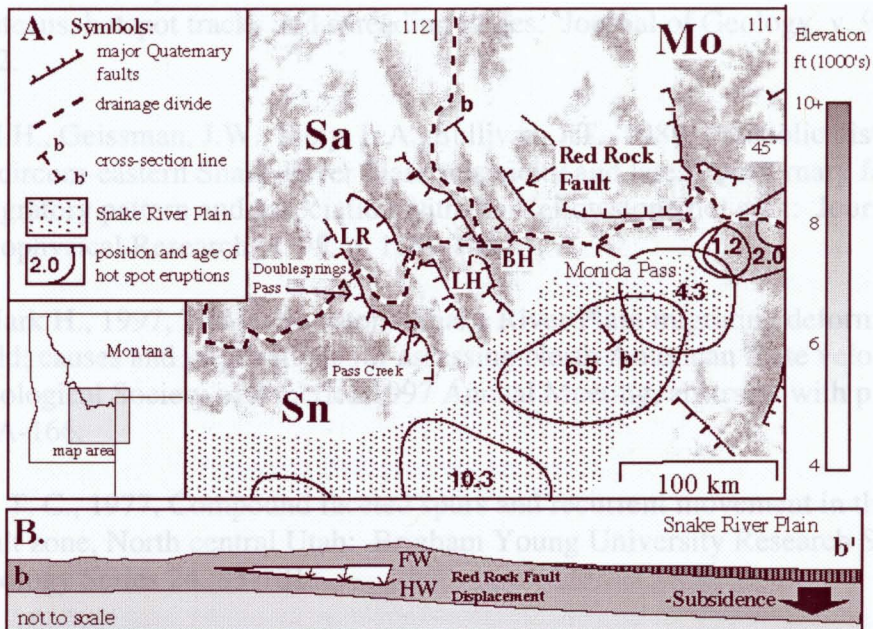


Figure 10

REFERENCES

- Alt, D., Sears, J.M., Hyndman, D.W., 1988, Terrestrial maria: The origins of large basalt plateaus, hotspot tracks and spreading ridges: *Journal of Geology*, v. 96, p. 647-662.
- Anders, M.H., Geissman, J.W., Piety, L.A., Sullivan, J.T., 1989, Parabolic distribution of circum-eastern Snake River Plain seismicity and latest Quaternary faulting; Migratory pattern and association with the Yellowstone hot spot: *Journal of Geophysical Research*, v. 95, p. 1589-1621.
- Anders, Mark H., 1997, The Yellowstone-Snake River Plain migrating deformation field; causes and implications for assessing North American Plate velocity: The Geological Society of America 1997 Annual Meeting, abstracts with programs, p. A-166.
- Anderson, T. C., 1977, Compound faceted spurs and recurrent movement in the Wasatch fault zone, North central Utah: *Brigham Young University Research Studies, Geology Series 24*, 83-101.
- Birkeland, Peter W., 1999, *Soils and Geomorphology*: New York, Oxford University Press, 430 p.
- Bull, William B., 1961, Tectonic significance of radial profiles of alluvial fans in western Fresno County, California: Article 75: U.S. Geological Society Professional Paper B182-B184.
- Bull, W. B. and McFadden, L.D., 1977, Tectonic geomorphology north and south of the Garlock fault, California: *in* Doerhing, D.O., ed., *Geomorphology of Arid Regions*. Proceedings of the Eighth Annual Geomorphology Symposium. State University of New York at Binghamton, p. 115-138.
- Christiansen, R.L., and McKee, E.H., 1979, Late Cenozoic volcanic and tectonic evolution of the Great Basin and Columbia Intermontane regions, *in* Smith, R.B., and Eaton, G.P., eds., *Cenozoic Tectonics and Geophysics of the Western Cordillera*: Boulder, Colorado, The Geological Society of America Memoir 152, p. 283-311.
- Cox, Randel T., 1994, Analysis of drainage basin symmetry as a rapid technique to identify areas of possible Quaternary tilt-block tectonics; an example from the Mississippi Embayment: *Geological Society of America Bulletin*, v. 106, n. 5, p. 571-581.

- Crone, A.J., and Haller, K.M., 1991, Segmentation and the coseismic behavior of Basin and Range normal faults: examples from east-central Idaho and southwestern Montana, USA: *Journal of Structural Geology* 13, no. 2, p. 151-164.
- Davis, John C., 1986, *Statistical and Data Analysis in Geology*: John Wiley and Sons, Inc., New York, 656 p.
- DePolo, Craig M., Clack, D.G., Slemmons B., and Ramelli, A. R., 1991, Historical surface faulting in the Basin and Range province, western North America: Implications for fault segmentation: *Journal of Structural Geology* 13, no. 2, p. 123-136.
- Dodge, R.L., and Grose, L.T., 1980, Tectonic and geomorphic evolution of the Black Rock Fault, northwestern Nevada: Proceedings of conference X; earthquake hazards along the Wasatch and Sierra Nevada frontal fault zones, U.S. Geological Survey Open-File Report 80-801, p. 494-508.
- Denny, Charles S., 1967, Fans and Pediments: *American Journal of Science*, v. 265, p. 81-105.
- Fields, R.W., Rasmussen, D.L., Tabrum, A.R., and Nichols, R., 1985, Cenozoic rocks of the intermontane basins of western Montana and eastern Idaho; a summary, *in* Flores, R.M., and Kaplan, S.S., eds., *Cenozoic paleogeography of the west central United States*: Rocky Mountain Section, Society of Economic Paleontologists and Mineralogists, Paleogeography Symposium 3, p. 9-36.
- Franklin, Steven E., 1987, Geomorphometric processing of digital elevation models; *Computers and Geosciences*, v. 13, n. 6, p. 603-609.
- Frankel, Kurt L., 2002, Quantitative topographic differences between erosionally exhumed and tectonically active mountain fronts: Implications for Late-Cenozoic evolution of the southern Rocky Mountains [M.S. thesis]: Lehigh University, 138 p.
- Fritz, W.J., and Sears, J.W., 1993, Tectonics of the Yellowstone hotspot wake in southwestern Montana: *Geology*, v. 21, p. 427-430.
- Gile, L.H., Peterson, F.F., and Grossman, R.B., 1966, Morphological and genetic sequences of carbonate accumulation in desert soils: *Soil Science*, v. 101, p. 347-360.
- Greenwell, Renee A. 1997. Alluvial fan development, the key to segmentation of the Red Rock fault, Southwestern Montana [M.S. Thesis]: University of South Carolina, ESRI dept., 71 p.

- Hack, J.T., 1973, Stream-profile analysis and stream-gradient index: U.S. Geological Survey Journal of Research, v. 1, p. 421-429.
- Haller, Kathleen M., 1988, Proposed segmentation of the Lemhi and Beaverhead faults, Idaho, and Red Rock fault, Montana--evidence from studies of fault scarp morphology: Geological Society of America Abstracts with Programs, v. 20, p. 418-419.
- Hamilton, Warren B., 1989, Crustal geologic processes of the United States, *in* Pakiser, L.C., and Mooney, W.D., eds., Geophysical framework of the continental United States: Boulder, Colorado, Geological Society of America Memoir 172, p. 743-781.
- Hare, P.W., and Gardner, T.W., 1985, Geomorphic indicators of vertical neotectonism along convergent plate margins, Nicoya Peninsula, Costa Rica: Tectonic Geomorphology, Binghamton Symposia in Geomorphology: International Series 15, p. 75-104.
- Hurlow, H.A., 1995, Structural style of Pliocene-Quaternary extension between the Red Rock and Blacktail faults, southwestern Montana, *in* Mogk, D.W., ed., Field guide to geologic excursions in southwest Montana: Northwest Geology 24, p. 221-228.
- Johnson, Peter P., 1981, Geology along the Red Rock fault and adjacent Red Rock Basin, Beaverhead County, Montana: Montana Geological Society 1981 Field Conference, SW Montana, p. 245-251.
- Klecker, Richard A., 1980, Paleozoic Sedimentology of the Dixon Mountain-Little water Canyon Area, Beaverhead County, Montana [Masters Thesis]: Oregon State University.
- Lonn, J.D., Skipp, B., Ruppel, E.T., Janecke, S.U., Perry, W.J., Sears, J.W., Bartholomew, M.J., Stickney, M.C., Fritz, W.J., Hurlow, H.A., and Thomas, R.C., 2000, Geologic map of the Lima 30' x 60' Quadrangle, Southwest Montana: Montana Bureau of Mines and Geology Open File 408, scale 1:100,000, 1 sheet.
- Lustig, L.K., 1965, Clastic sedimentation in Deep Springs Valley, California: U.S. Geological Survey Professional Paper 352-F.
- McCalpin, James P., 1996, Paleoseismology in extensional tectonic environments: Paleoseismology, International Geophysics Series, v. 62, p. 85-146.

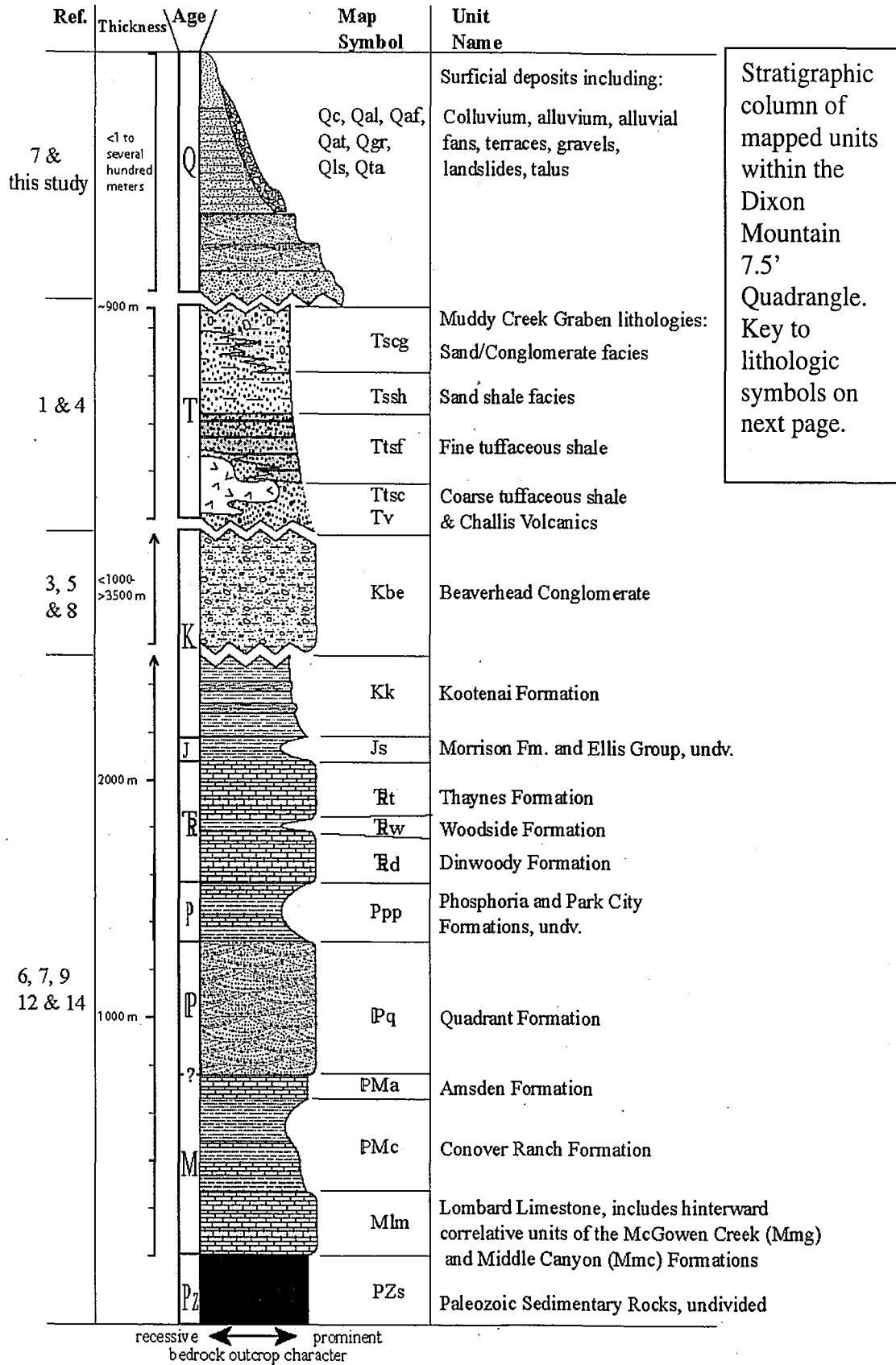
- McDowell, Robin J., 1989, Effects of Syn-Sedimentary Basement Tectonics on Fold Thrust Geometry, Southwestern Montana [Ph.D. Dissertation]: University of Kentucky, Lexington.
- McQuarrie, Nadine, and Rodgers, David W., 1998, Subsidence of a volcanic basin by flexure and lower crustal flow: The eastern Snake River Plain, Idaho: *Tectonics*, v. 17, n. 2, p. 203-220.
- Morgan, W. J., 1972, Plate motions and deep mantle convection: *Memoir of the Geological Society of America* 132, p. 7-22.
- Parsons, T., Thompson, G.A., Sleep, N.H., 1994, Mantle plume influence on the Neogene uplift and extension of the U.S. western Cordillera?: *Geology*, v. 22, p. 83-86.
- Pierce, K.L. and Morgan, L.A., 1992, The track of the Yellowstone hot spot: Volcanism, faulting, and uplift, *in* Link, P.K., Kuntz, M.A., and Platt, L.B., eds., *Regional geology of Eastern Idaho and Western Wyoming*: Geological Society of America Memoir 179.. p. 1-51.
- Pierce, J.L., and Meyer, G.A., 2001, Using evidence of fires in alluvial fan stratigraphy to interpret variations in Holocene fire regimes in central Idaho; *Geological Society of America*, abstracts with programs 33, n. 6, p. 69.
- Pike, R.J., and Wilson, S.E., 1971, Elevation-relief ratio, hypsometric integral, and geomorphic area-altitude analysis: *Geological Society of America Bulletin*, v. 82, p. 1079-1084.
- Reheis, M. C., 1987, Soils in granitic alluvium in humid and semi-arid climates along Rock Creek, Carbon County, Montana: *U.S. Geological Survey Bulletin* 1590-D, 41p.
- Ritter, J.B., Miller, J.R., Enzel, Y., Howes, S.D., Nadon, G., Grubb, M.D., Hoover, K.A., Olsen, T., Reneau, S.L., Sack, D., Summa, C.L., Taylor, I., Touyinhthiphonexay, K.C.N., Yodis, E.G., Schneider, N.P., Ritter, D.F., and Wells, S.G., 1993, Quaternary evolution of the Cedar Creek Alluvial Fan, Montana: *Geomorphology*, v. 8, p. 287-304.
- Rodgers, D. W., Hackett, W.R., and Ore, H.T., 1990, Extension of the Yellowstone plateau, eastern Snake River Plain, and Owyhee plateau: *Geology*, v. 18, p. 1138-1141.

- Scholten, Robert K., Keenmon, K.A., and Kupsch, W.O., 1955, Geology of the Lima region, Southwestern Montana and adjacent Idaho: Geological Society of America Bulletin, v. 66, p. 345-404.
- Schwartz, D.P., Swan, F.H., III, Hanson, K.L., 1982, Fault zone segmentation based on geometry and recurrence; the Wasatch fault zone, Utah: Seismological Society of America, abstracts, Earthquake Notes, v. 54, n. 1, p. 60.
- Smith, R.B., and Sbar, M.L. 1974, Contemporary Tectonics and Seismicity of the Western United States with Emphasis on the Intermountain Seismic Belt: Geological Society of America Bulletin, v. 85. p. 1205-1218.
- Smith, R.B., Nagy, W.C., Julander, K.A., Viveiros, J.J., Barber, C.A., and Gants, D.G., 1989, Geophysical and tectonic framework of the eastern Basin and Range-Colorado Plateau-Rocky Mountain transition, *in* L.C. Pasker and W.D. Mooney, eds., Geophysical framework of the continental United States: Memoir of the Geological Society of America 172, p. 205-233.
- Stein, R.S., and Barrientos, S.E., 1985, The 1983 Borah Peak, Idaho, earthquake; geodetic evidence for deep rupture on a planar fault, *in* Stein, R.S., and Bucknam, R.C., eds., Proceedings of Workshop XXVII on the Borah Peak, Idaho, earthquake: U.S. Geological Survey Open-File Report 85-290, p. 76-96.
- Stickney, M.C., and Bartholomew, M.J., 1987, Seismicity and late Quaternary faulting of the Northern Basin and Range province, Montana and Idaho: Bulletin of the Seismological Society of America, v. 77, n. 5, p. 1602-1625.
- Stickney, M.C., Bartholomew, M.J., and Wilde, E.M. 1987, Trench logs across the Red Rock, Blacktail, Lima Reservoir, Georgia Gulch, Vendome and Divide faults, Montana: Geological Society of America, Rocky Mtn. Section, 40th Annual Meeting Abstracts with Programs, v. 19, no. 5. 336-337.
- Stickney, M.C., and Lageson, D.R., 2002, Seismotectonics of the 20 August 1999 Red Rock Valley, Montana, Earthquake: Bulletin of the Seismological Society of America, v. 92, n. 6, p. 2449-2464.
- Strahler, A.N., 1952, Hypsometric (area-altitude) analysis of erosional topography: Geological Society of America Bulletin, v. 63, p. 1117-1142.
- Turko, Julianne M. and Knuepfer, Peter L.K., 1991, Late Quaternary fault segmentation from analysis of scarp morphology: Geology, v. 19, n. 7, p. 718-721.


- Wells, D.J., and Coppersmith, K.J., 1994, New empirical relationships among magnitude, rupture length, rupture width, rupture area, and surface displacement: Bulletin of the Seismological Society of America 84, n. 4, p. 974-1002.
- Wheeler, Russell L., 1987, Boundaries between segments of normal faults; criteria for recognition and interpretation *in* Proceedings of Conference XXXIX; directions in paleoseismology: open file report, U.S. Geological Survey, p. 385-398.
- Williams, Nancy S. 1984, Stratigraphy and structure of the east-central Tendo Range, Southwestern Montana [Masters Thesis]: University of North Carolina, Chapel Hill.
- Zhang, P., Slemmons, D.B., and Mao, F., 1991, Geometric pattern, rupture termination and fault segmentation of the Dixie Valley-Pleasant Valley active normal fault system, Nevada, U.S.A.: Journal of Structural Geology, v. 13, n. 2, p. 165-176.
- Zoback, M.L., and Zoback, M.D., 1989, Tectonic stress field of the continental United States: Geophysical framework of the continental United States, Geological Society of America Memoir 172, p. 523-539.


**Appendix: Bedrock and Surficial Geologic Map
Dixon Mountain 7.5' Quadrangle**


Note: This appendix includes the surficial and bedrock map of the Dixon Mountain 7.5' Quadrangle (in back pocket), accompanying stratigraphic descriptions and legend, and two brief notes describing significant structural relationships observed while compiling the map sheet. The map and notes were submitted as open file reports to the Montana Bureau of Mines and Geology (MBMG) and the United States Geological Survey (USGS) as part of the DOI EDMAP/STATEMAP program.




Key to lithologic symbols on stratigraphic column.

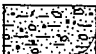
 Sand & conglomerate


 Sand & shale

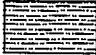
 Fine Tuffaceous shale
and ash


 Coarse tuffaceous shale
and ash


 Basalt and andesite

 Cobble to boulder
Conglomerate

 Cross-bedded to
massive sandstone

 Shale and mudstone

 Limy shale and
Limestone

 Limestone

Legend and Unit Description

Quaternary

- Qal *Alluvium*: Unconsolidated, sorted to poorly sorted deposit of fluvial silt, sand, and gravel, in and at grade with modern stream and channels.
- Qaf₁ *Youngest alluvial fan deposit*: Fan-shaped deposit of unconsolidated alluvial gravel sand and silt. Relative age within the map area assigned based on surface morphology
- Qaf₂ *Older Alluvial fan deposit*: Fan shaped deposit of unconsolidated alluvial gravel, sand, and silt. Delineated as the oldest within the map area based on surface morphology
- Qafo *Old alluvial fan deposit*: Deposit of unconsolidated boulders, gravel, sand, and silt, usually fan-shaped, often dissected and found several tens of meters higher than adjacent modern alluvium. Relative age uncertain but likely older than Qaf₂.
- Qat₁ *Youngest terrace*: Deposits of fluvial silt, sand, and gravel with a characteristic flat-topped "tread" morphology; multiple tread surfaces are observed, often well sorted and bedded. Continuous surfaces are assigned relative ages according to elevation above modern alluvium, Qat₁ is the youngest, preserved at 1-3 meters above modern channels.
- Qat₂ *Second youngest terrace*: Terrace deposits preserved at 5-10 meters above modern channels.
- Qat₃ *Oldest terrace*: Generally isolated terrace deposits preserved at 12-15 meters above modern channels.
- Qls *Landslides*: Unconsolidated deposits of locally derived, angular, unsorted debris with a characteristic hummocky topography and head scarp.
- Qc *Colluvium*: Thick unconsolidated hillslope, talus, and rockfall deposits; contains some alluvium. Grain size ranges from boulder to silt, clasts are often angular to semi-angular.
- Qta *Talus*: hillslope deposits of unsorted, angular rock fragments.
- Qg *Gravels*: Isolated, thick deposits of unconsolidated, rounded gravels and sands, clasts composed of quartzite, sandstone, limestone, and a variety of igneous lithologies

Quaternary-Tertiary

QTgr *Gravels*: Isolated, thick deposits of unconsolidated, rounded gravels and sands that are likely significantly older than similar units mapped as gravels.

Tertiary

- Tscg *Sand / conglomerate facies*: Conglomerates and sandstones with multiple depositional features including cross-bedding, scour fill, and horizontal bedding. Contains cobbles of Tendoy thrust sheet affinity.
- Tssh *Shale / sand facies*: Variegated, buff to rusty sandstones, mudstones, shales, and rare limestones, often thin-bedded and fossiliferous.
- Ttsf *Tuffaceous sediment, fine*: Predominantly buff-colored tuffaceous sandstones and siltstones, some limestones and marls, thinly laminated and usually lacking fossils; significant ash content.
- Ttsc *Tuffaceous sediment, coarse*: Variegated buff to brown-colored, tuffaceous sediments that retain most of their original pyroclastic character; mostly sandy but conglomeratic in places.
- Tv *Volcanic rocks*: massive basalt and andesite, basaltic agglomerate and rhyolite tuff. Often black, dark brown, to dark red in color.

Tertiary-Cretaceous

Kbe *Beaverhead conglomerate (as observed at the top of Little Water Canyon)*: Reddish conglomerate with clasts ranging from 1 meter to sand size; cobbles composed of limestone, chert, sandstone, and quartzite, mostly massive with some finer sand and silt lenses and beds.

Cretaceous

Kk *Kootenai Formation*: Predominantly reddish-colored, thinly-bedded sandstone and siltstone; contains "salt and pepper" sandstone beds and lacustrine limestone; cherty conglomerate at base. Undifferentiated units of the Frontier and Blackleaf Formations.

Jurassic

- Js *Jurassic sedimentary rocks undivided (Morrison and Ellis Group, undivided):* Nonmarine to marine siltstones, sandstones, calcareous siltstones, and limestones. Seldom outcrop and are never prominent.

Triassic

- Trt *Thaynes Formation:* Marine, light gray-weathering to buff-colored, thin-bedded and laminated, fossiliferous, silty limestone; locally contains black chert; cliff-forming.
- Trw *Woodside Formation:* Rusty to tan-colored, transitional marine, fenestrial silty limestone, calcareous siltstone and sandstones; rarely exposed.
- Trd *Dinwoody Formation:* Marine, dark rusty to dark "chocolate" brown, thin-bedded calcareous siltstone and fossiliferous silty limestone; cliff-forming.

Permian

- Ppp *Phosphoria and Park City Formations, undivided:* Marine, light colored phosphatic shale, calcareous siltstone and sandstone, and fossiliferous limestone.

Pennsylvanian

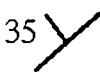


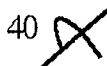

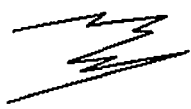
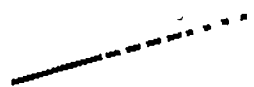



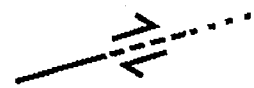
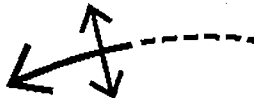

- IPq *Quadrant Formation:* Buff-colored, cliff-forming, thick-bedded to massive, cross-bedded, calcareous sandstone to pure sandstone.

Mississippian

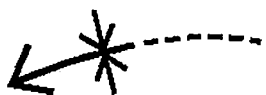
- IPMa *Amsden Formation:* Light to dark gray, weathers to brown, marine thin-bedded fossiliferous limestone and calcareous sandstone, with basal limestone conglomerate.
- IPMrc *Conover Ranch Formation:* Buff-colored, cross-bedded sandstone, finely inter-bedded sandstone and siltstones, rhythmically bedded black shales, and some light to dark gray, thin-bedded fossiliferous limestone.
- Mlm *Lombard Formation (as observed at Deadwood Gulch):* Light to dark gray, thin-bedded, fossiliferous limestones, inter-bedded with buff, calcareous siltstone.

Pzs *Paleozoic sedimentary rocks, undivided*: Paleozoic limestones and clastic rocks of unknown formation affinity, although most likely the Middle Canyon and Lombard Formations.

Map Symbols

35 	Bedding strike and dip where measured
	Horizontal bedding
	Vertical bedding
40 	Overturned bedding
	Contact; dashed where approximate, dotted where concealed
	Facies change in sedimentary rocks
	Fault with unknown sense of movement; dashed where approximate; dotted where concealed
	Normal fault; ball and bar on downthrown or hanging wall side; dashed where approximate; dotted where concealed
	Thrust or reverse fault; teeth on hanging wall side; dashed where approximate; dotted where concealed
	Detachment fault, normal sense; symbols on hanging wall; dashed where approximate; dotted where concealed
	Strike-slip fault; dashed where approximate; dotted where concealed
	Axial trace of anticline showing plunge; dashed where approximate
	Axial trace of overturned anticline showing plunge; dashed where approximate

Map Symbols Continued



Axial trace of syncline showing plunge; dashed where approximate



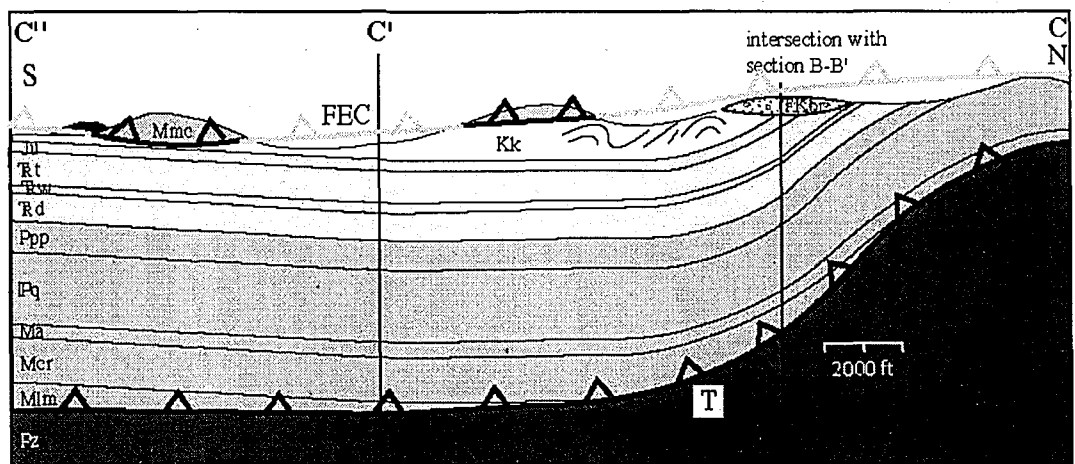
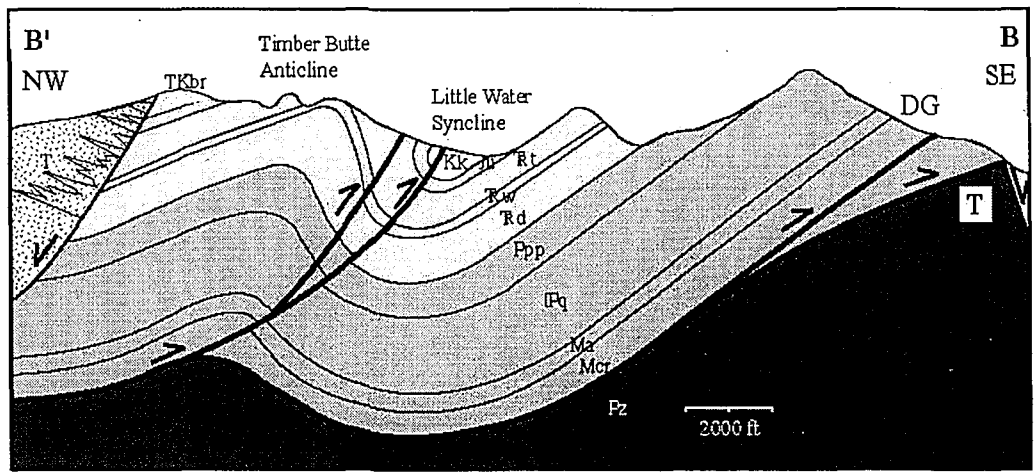
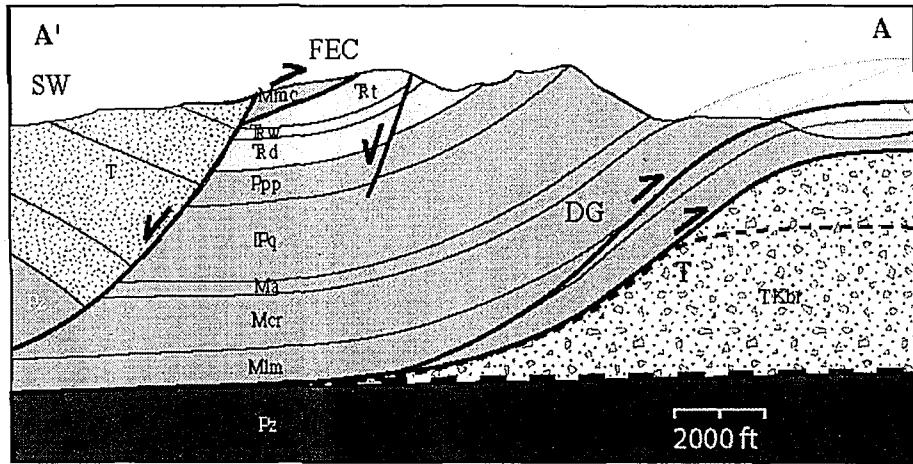
Axial trace of overturned syncline showing plunge: dashed where approximate



Fold train and axial strike



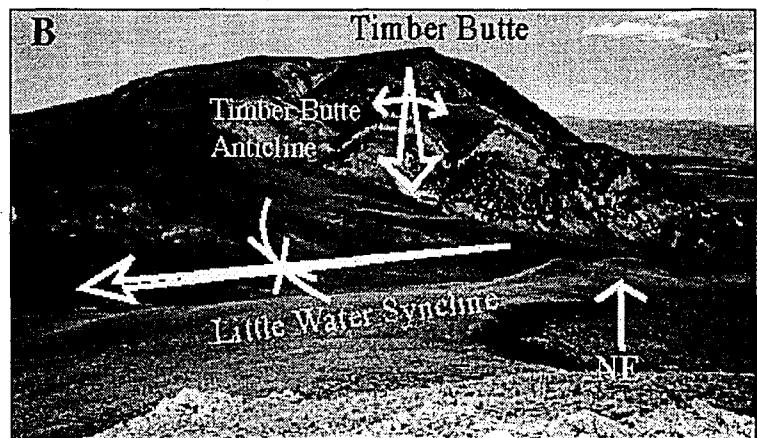
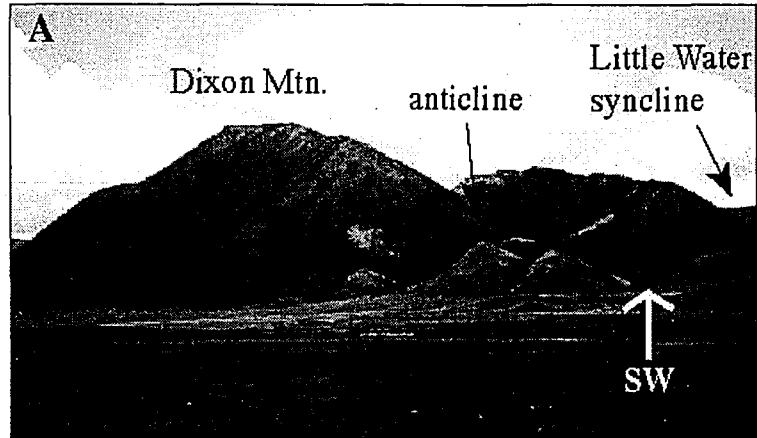
Fault scarp



Thrust abbreviations: (T) Tendoy, (DG) Deadwood Gulch, (FEC) Four Eyes Canyon
 Interpreted cross sections.

Map Note 1. Transverse folding in the Tendoy Thrust Sheet as a result of interactions with complex footwall geometry

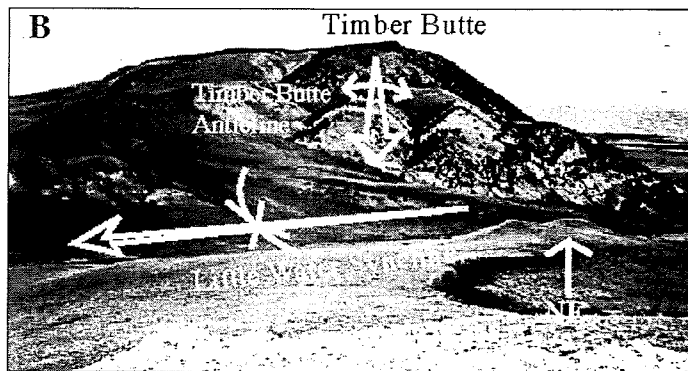
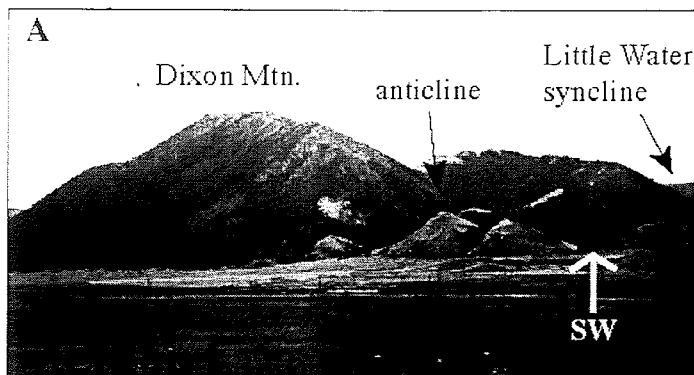
The Tendoy Thrust Sheet, the frontal Sevier thrust in the Tendoy Mountains, exhibits footwall and hanging wall ramp and flat geometries commonly observed in frontal thrust sheets. Folds observed around section 10, T. 13 S., R. 10 W., the Timber Butte anticline and Little Water syncline, are transport-parallel, kilometer scale transverse folds in the Tendoy thrust sheet. Picture A at right (right) is a view to the southwest of the eastern front of the Tendoy Range in which the folding can be seen. Fold hinges trend SW-NE and



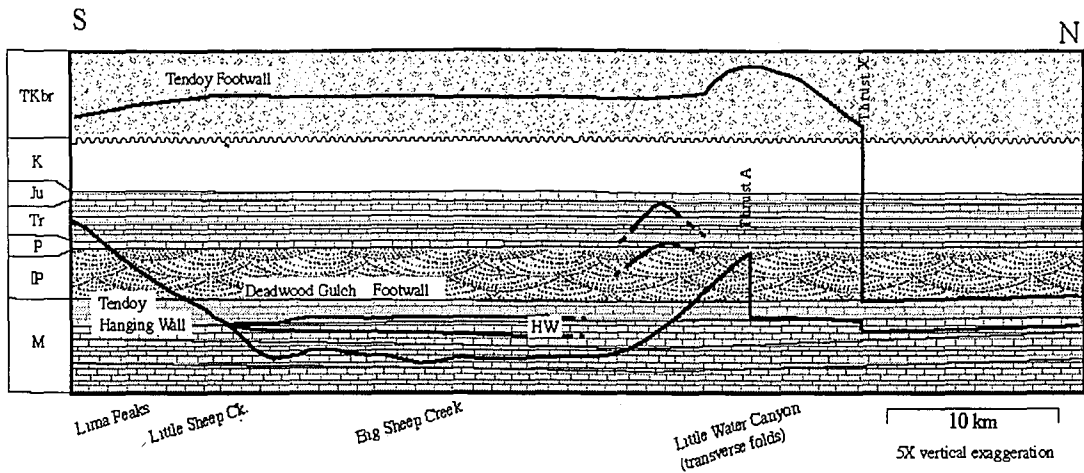
plunge steeply ($>20^\circ$) towards the hinterland, as a result of interaction with a frontal footwall ramp. The trend and plunge of the fold axis are visible in picture B, which displays a view looking northeast from the top of the Little Water Canyon drainage. Units in the northern limb of the Little Water syncline (south limb of the Timber Butte anticline) are overturned. Also at this location, a SW-NE-striking thrust originates from the syncline hinge and increases its offset towards the foreland. The hanging wall ramp observed proximal to these folds suggests they developed coincident to emplacement of the Tendoy thrust sheet (stratigraphic separation diagram, next page), potentially as a result of interactions with an oblique or lateral footwall ramp geometry. These folds have been previously explained as pre-thrusting structures, associated with uplift of the nearby Blacktail-Snowcrest Laramide

Map Note 1. Transverse folding in the Tendoy Thrust Sheet as a result of interactions with complex footwall geometry

The Tendoy Thrust Sheet, the frontal Sevier thrust in the Tendoy Mountains, exhibits footwall and hanging wall ramp and flat geometries commonly observed in frontal thrust sheets. Folds observed around section 10, T. 13 S., R. 10 W., the Timber Butte anticline and Little Water syncline, are transport-parallel, kilometer scale transverse folds in the Tendoy thrust sheet. Picture A at right (right) is a view to the southwest of the eastern front of the Tendoy Range in which the folding can be seen. Fold hinges trend SW-NE and



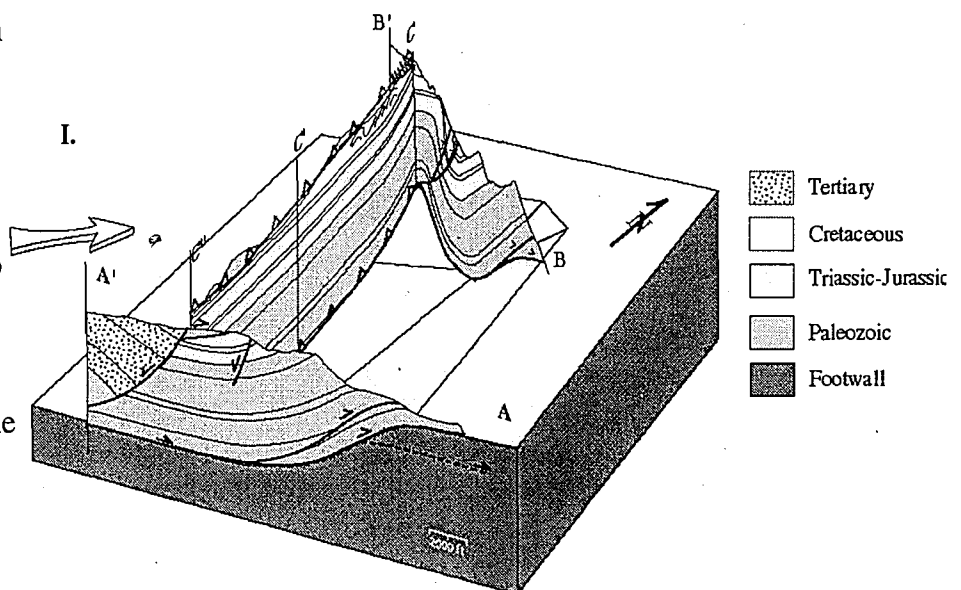
plunge steeply ($>20^\circ$) towards the hinterland, as a result of interaction with a frontal footwall ramp. The trend and plunge of the fold axis are visible in picture B, which displays a view looking northeast from the top of the Little Water Canyon drainage. Units in the northern limb of the Little Water syncline (south limb of the Timber Butte anticline) are overturned. Also at this location, a SW-NE-striking thrust originates from the syncline hinge and increases its offset towards the foreland. The hanging wall ramp observed proximal to these folds suggests they developed coincident to emplacement of the Tendoy thrust sheet (stratigraphic separation diagram, next page), potentially as a result of interactions with an oblique or lateral footwall ramp geometry. These folds have been previously explained as pre-thrusting structures, associated with uplift of the nearby Blacktail-Snowcrest Laramide



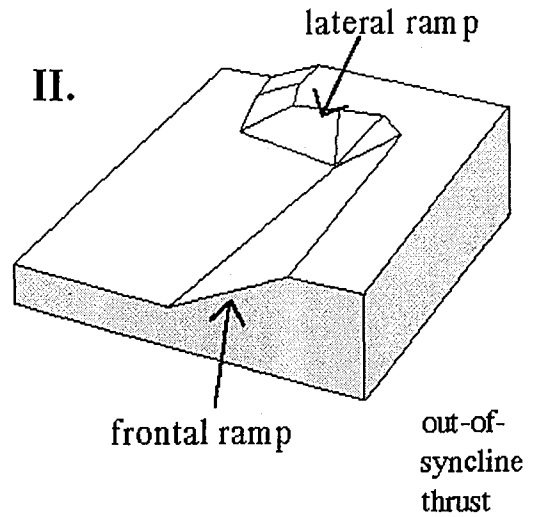
(Above) Stratigraphic separation diagram of the Tendoy and Deadwood Gulch thrust sheets. At its southern extreme, the Tendoy hanging wall cuts rapidly down section, attaining a flat within the Mississippian Lombard Fm.^{8,9} The Deadwood Gulch thrust is an out-of-sequence imbricate of the Tendoy, carrying a flat in the Mississippian Conover Ranch Fm., with little stratigraphic separation. The Tendoy hanging wall laterally ramps up through the Upper Paleozoic section in the vicinity of the transverse folds, evidence of lateral ramp development at the base of the hanging wall. Further north, two small thrusts (likely imbricates³) complicate geometry. At the northern extent of the Tendoy Sheet stratigraphic separation is small, with both the hanging wall and footwall of the thrust residing completely within Mississippian stratigraphy.

(Below) Three cross sections through the Dixon Mountain quadrangle illustrate the three-dimensional structure of the Tendoy thrust sheet and potential underlying footwall oblique ramp geometry. The sections (A-A', B-B', and C-C'-C'') are delineated on the accompanying map sheet. Approximate transport direction is indicated by the arrow at

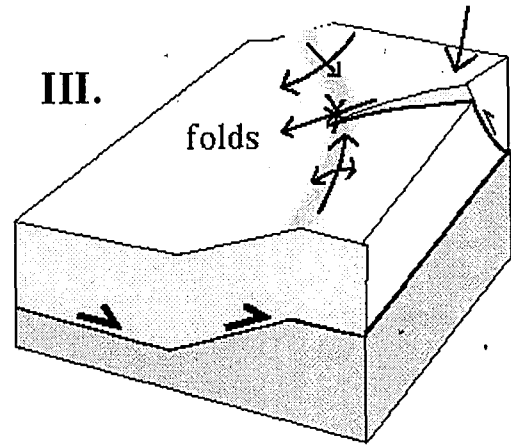
top left. Note in section B-B', which trends laterally across the folds and nearly perpendicular to the transport direction, the interpreted fold geometry and the out-of-the-syncline thrust.



(Right) Block diagram displaying the simplified interpreted footwall ramp geometry. The frontal ramp steps westward, creating an oblique ramp and corner in the vicinity of the Little Water and Timber Butte Folds (upper part of block diagram).

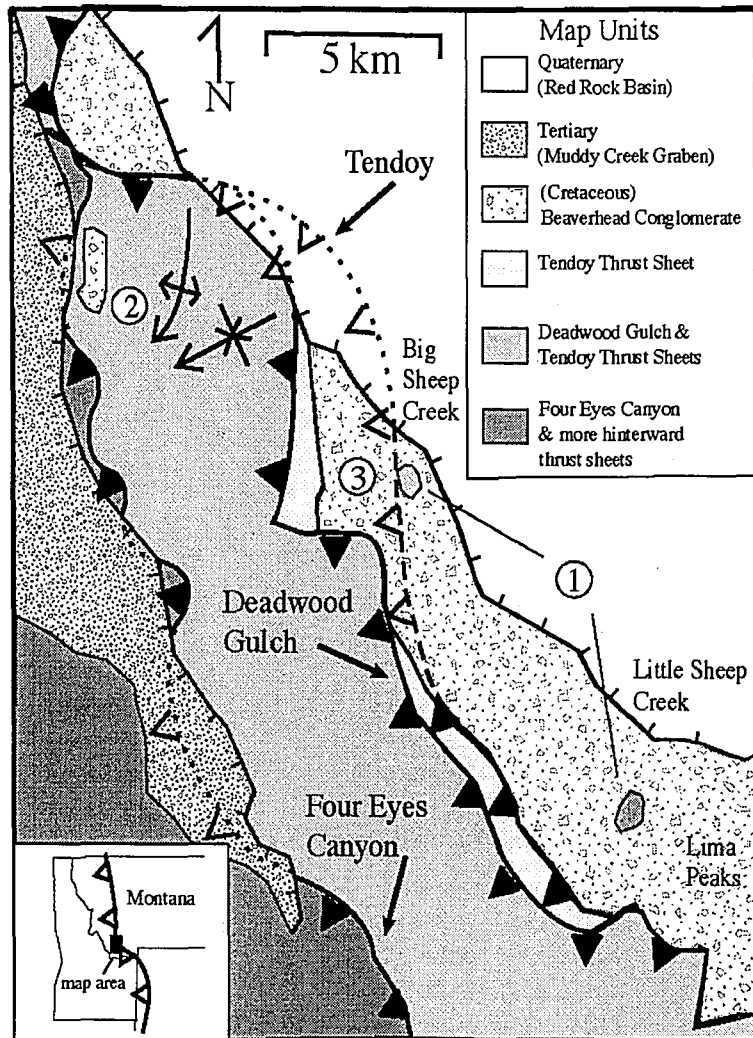


Emplacement of a thrust sheet over the lateral ramp diagrammed in figure II. would lead to the development of transverse, hinterward plunging folds. Space constraints in the ramp corner are accommodated by an out-of-the-syncline thrust.

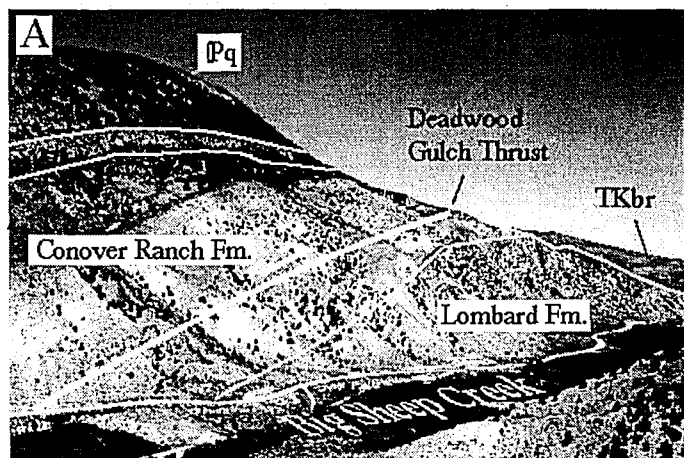


Map Note 2. Constraints on the emplacement chronology of the Tendoy, Deadwood Gulch, and Four Eyes Canyon Thrust Sheets.

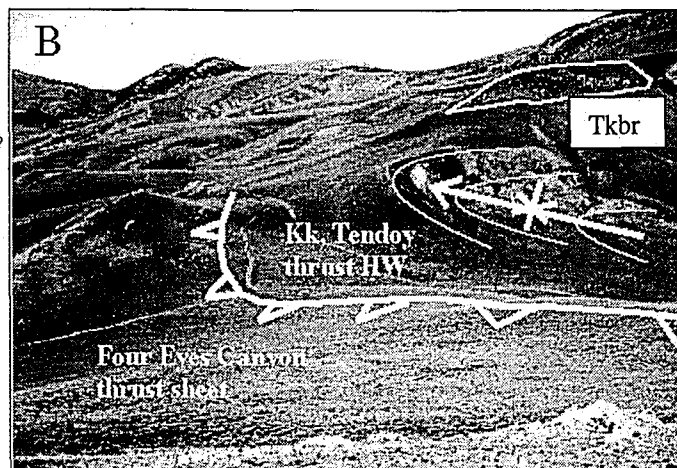
(Right) A simplified map of the present position of the frontal thrust sheets in the Tendoy Mountains⁷. Circled numbers are keyed to the text, thrust positions are dashed where covered and approximated, dotted where truncated. The spatial and structural relationships of these thrust sheets to each other along with widespread deposits of Cretaceous synorogenic conglomerates of the Beaverhead Group help to constrain the emplacement chronologies of the frontal thrust sheets in the Dixon Mountain 7.5' Quadrangle.



(Lower right) Photo A displays exposures along the northern bank of Big Sheep Creek (map location 3). Here the Tendoy Sheet is unconformably overlain by synorogenic Beaverhead Conglomerate (TKbr). The Deadwood Gulch thrust repeats the Conover Ranch Formation, and emplaces Paleozoic units over the Tendoy sheet and associated Beaverhead deposits.



In photo **B**, taken looking to the north at the head of Little Water Canyon (map location 2), an exposure of synorogenic conglomerate contains boulders of Four Eyes Canyon thrust sheet affinity emplaced unconformably over tightly folded units in the Tendoy sheet. The Four Eyes Canyon sheet subsequently overrode these syn-orogenic deposits and the folded Tendoy sheet units, to be folded later by late-stage Tendoy sheet activity.



Field Relationships

Structural relationships mapped in and around the Dixon Mountain Quadrangle provide constraints on the timing of Sevier frontal thrust sheet emplacement in the Tendoy Mountains. Depositional relationships within the Beaverhead Conglomerate, a Cretaceous syn-orogenic package of sediment sourced off of emergent thrust sheets¹⁰, record the relative emplacement timing of the Tendoy, Deadwood Gulch, and Four Eyes Canyon thrusts during the Late Cretaceous⁵. The following field relationships are observed:

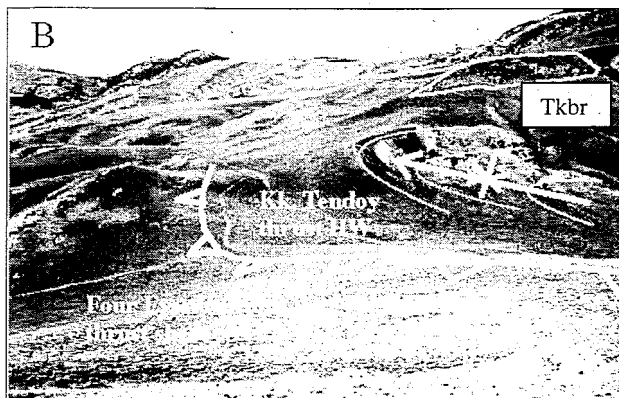
Olistostromes within local exposures of Beaverhead conglomerate help to establish sediment affinities (map location 1). In the south, an olistostrome was sourced from the Four Eyes Canyon thrust sheet¹⁰. Farther north, another block appears to have been sourced from an emergent Deadwood Gulch thrust.

The Tendoy thrust was both emplaced over, and blanketed by Beaverhead Conglomerate. Along Big Sheep Creek (map location 2), the Tendoy sheet is blanketed by Beaverhead units sourced from the Deadwood Gulch thrust.

The Deadwood Gulch thrust is emplaced over the top of the Tendoy sheet and associated Beaverhead Units, potentially sourcing the northern olistostrome.

In Little Water Canyon (map location 3), syn-orogenic conglomerate is synthetically sourced from an emergent Four Eyes Canyon sheet, and emplaced over the top of tightly folded units in the Tendoy thrust sheet.

In photo **B**, taken looking to the north at the head of Little Water Canyon (map location 2), an exposure of synorogenic conglomerate contains boulders of Four Eyes Canyon thrust sheet affinity emplaced unconformably over tightly folded units in the Tendoy sheet. The Four Eyes Canyon sheet subsequently overrode these syn-orogenic deposits and the folded Tendoy sheet units, to be folded later by late-stage Tendoy sheet activity.



Field Relationships

Structural relationships mapped in and around the Dixon Mountain Quadrangle provide constraints on the timing of Sevier frontal thrust sheet emplacement in the Tendoy Mountains. Depositional relationships within the Beaverhead Conglomerate, a Cretaceous syn-orogenic package of sediment sourced off of emergent thrust sheets¹⁰, record the relative emplacement timing of the Tendoy, Deadwood Gulch, and Four Eyes Canyon thrusts during the Late Cretaceous⁵. The following field relationships are observed:

Olistostromes within local exposures of Beaverhead conglomerate help to establish sediment affinities (map location 1). In the south, an olistostrome was sourced from the Four Eyes Canyon thrust sheet¹⁰. Farther north, another block appears to have been sourced from an emergent Deadwood Gulch thrust.

The Tendoy thrust was both emplaced over, and blanketed by Beaverhead Conglomerate. Along Big Sheep Creek (map location 2), the Tendoy sheet is blanketed by Beaverhead units sourced from the Deadwood Gulch thrust.

The Deadwood Gulch thrust is emplaced over the top of the Tendoy sheet and associated Beaverhead Units, potentially sourcing the northern olistostrome.

In Little Water Canyon (map location 3), syn-orogenic conglomerate is synthetically sourced from an emergent Four Eyes Canyon sheet, and emplaced over the top of tightly folded units in the Tendoy thrust sheet.

Units in the Four Eyes Canyon sheet truncate the kilometer-scale transverse folds of the Little Water syncline and Timber Butte anticline.

Deformation within Beaverhead units is associated with late-stage activity of a lower, more frontal detachment (possibly the Lima Thrust)¹⁰.

Deformation Sequence Schematic

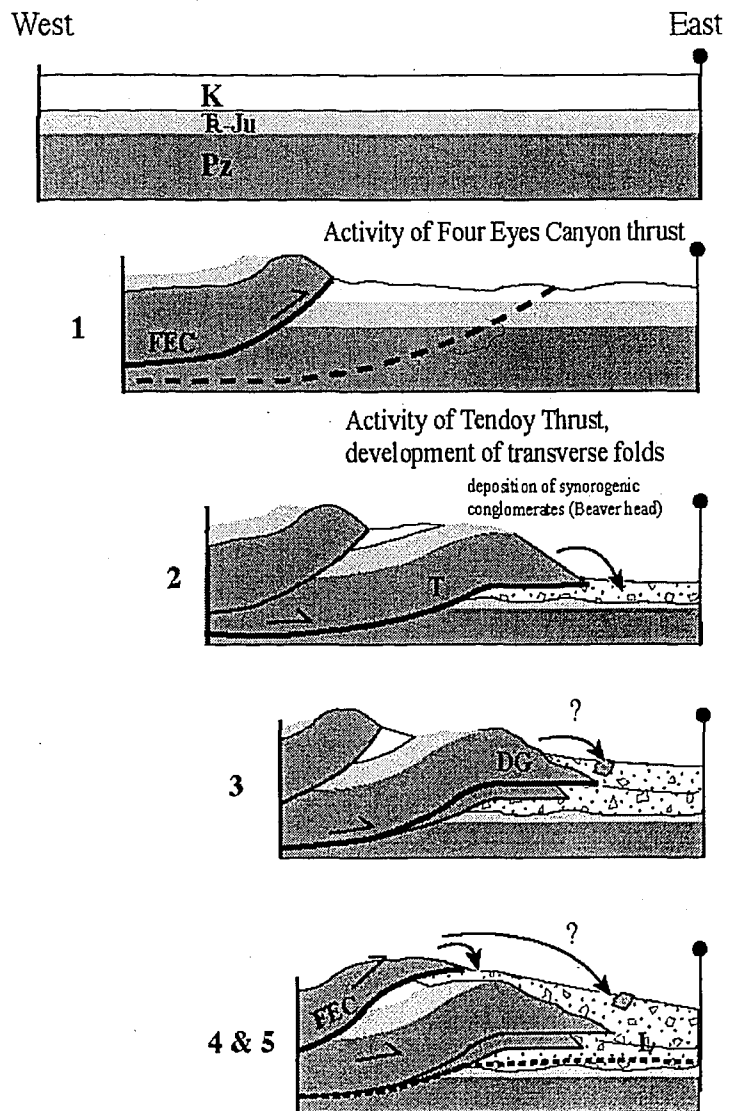
Field relationships allow for the construction of a schematic diagram of potential emplacement chronology, illustrated at right

1. Early activity of the Four Eyes Canyon thrust (FEC).

2. Emergent activity of the Tendoy sheet (T), deposition of associated syn-orogenic sediment, early development of transverse folds.

3. Out-of-sequence, emergent activity of the Deadwood Gulch thrust (DG), antithetic and synthetic deposition of Beaverhead, sourcing of olistotromes.

4. Out-of-sequence emergent activity of the Four Eyes thrust, deposition of syn-orogenic sediments onto the foreland and Tendoy hanging wall.



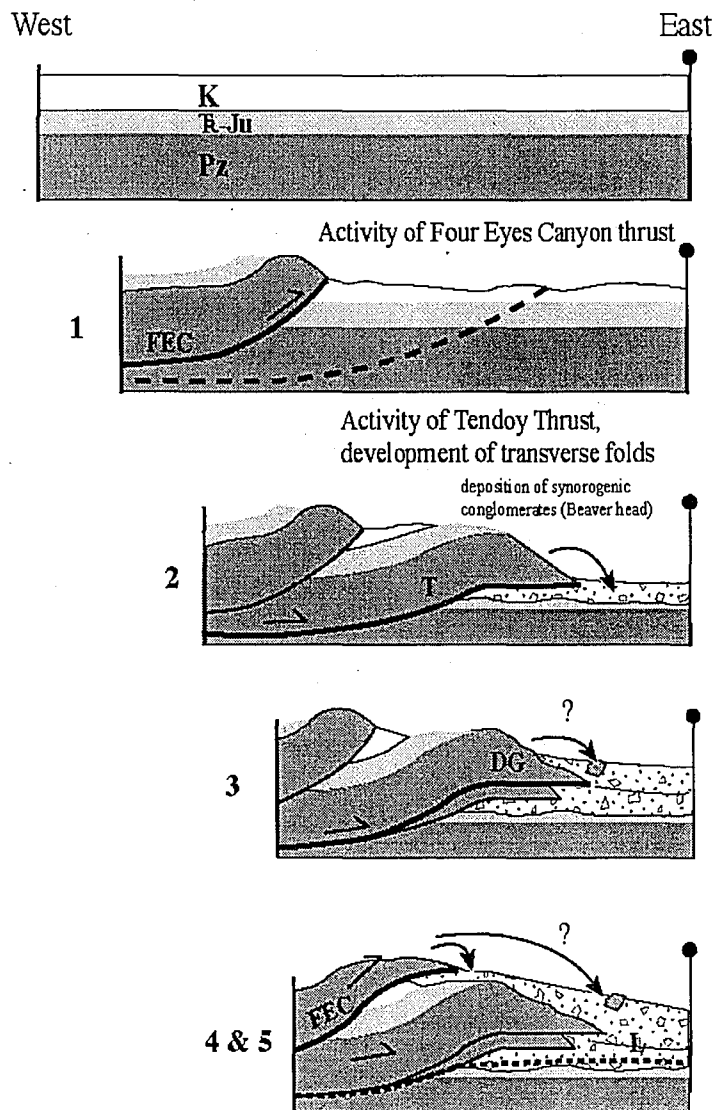
Units in the Four Eyes Canyon sheet truncate the kilometer-scale transverse folds of the Little Water syncline and Timber Butte anticline.

Deformation within Beaverhead units is associated with late-stage activity of a lower, more frontal detachment (possibly the Lima Thrust)¹⁰.

Deformation Sequence Schematic

Field relationships allow for the construction of a schematic diagram of potential emplacement chronology, illustrated at right

1. Early activity of the Four Eyes Canyon thrust (FEC).
2. Emergent activity of the Tendoy sheet (T), deposition of associated syn-orogenic sediment, early development of transverse folds.
3. Out-of-sequence, emergent activity of the Deadwood Gulch thrust (DG), antithetic and synthetic deposition of Beaverhead, sourcing of olistotromes.
4. Out-of-sequence emergent activity of the Four Eyes thrust, deposition of syn-orogenic sediments onto the foreland and Tendoy hanging wall.



Works cited in appendix A

1. Dunlap, Dennis G., 1982, Tertiary geology of the Muddy Creek basin, Beaverhead County, MT: M.S. thesis, University of Montana, Missoula.
2. Greenwell, Renee A., 1997, Alluvial fan development, the key to segmentation of the Red Rock fault, Southwestern Montana: M.S. Thesis, University of South Carolina, ESRI dept. 71 p.
3. Haley, Christopher, 1986, Upper Cretaceous (Beaverhead) synorogenic sediments in the Montana, Idaho thrust belt and adjacent foreland: Relationships between sedimentation and tectonism: The Johns Hopkins University, Baltimore MD, PhD. dissertation, 452 p.
4. Janecke, S., McIntosh, W., and Good, S., 1999, Testing models of rift basins: structure and stratigraphy of an Eocene-Oligocene supradetachment basin, Muddy Creek half graben, south-west Montana. Basin Research 11, p 143-165.
5. Kalakay, T.J., 1997, Large scale magmatism during development of a thin-skinned fold and thrust wedge; examples from the Pioneer Batholith, Southwest Montana, and Venusiam Coronae. Geological Society of America Abstracts with programs v. 29, no. 6, p. 222-223.
6. Klecker, Richard A., 1980, Paleozoic Sedimentology of the Dixon Mountain-Little water Canyon Area, Beaverhead County, Montana: Oregon State University, MS Thesis.
7. Lonn, J.D., Skipp, B., Ruppel, E.T., Janecke, S.U., Perry, W.J., Sears, J.W., Bartholomew, M.J., Stickney, M.C., Fritz, W.J., Hurlow, H.A., and Thomas, R.C., 2000, Geologic map of the Lima 30' x 60' Quadrangle, Southwest Montana. Montana Bureau of Mines and Geology open file report 408 scale 1:100,000.
8. McDowell, Robin J., 1989, Effects of Syn-Sedimentary Basement Tectonics on Fold Thrust Geometry, Southwestern Montana: University of Kentucky, Lexington, Ph.D Dissertation.
9. McDowell, Robin J., 1997, Evidence for synchronous thin-skinned and basement deformation in the Cordilleran fold-thrust belt: the Tendoy Mountains, southwestern Montana. Journal of Structural Geology v. 19, p. 77-87.

10. Perry, W.J. & Sando, W.J., 1983, Sequential deformation in the thrust belt of southwestern Montana. *In*: Powers, R.B., ed., Geologic studies of the Cordilleran Thrust Belt, Rocky Mountain Association of Geologists, v.1, p. 137-144.
11. Ponton, J.D., 1983, Structural analysis of the Little Water syncline, Beaverhead County, Montana: Texas A&M University, MS Thesis.
12. Scholten, Robert K., Keenmon, K.A., and Kupsch, W.O., 1955, Geology of the Lima region, Southwestern Montana and adjacent Idaho. Geological Society of America Bulletin v. 66, p. 345-404.
13. Skipp, Betty S., 1988, Cordilleran thrust belt and faulted foreland in the Beaverhead Mountains, Idaho and Montana, Geological Society of America Memoir no. 171.
14. Williams, Nancy S., 1984, Stratigraphy and structure of the east-central Tendoy Range, Southwestern Montana: University of North Carolina, Chapel Hill, MS Thesis.

VITA

Nathan Ward Harkins

Date/Place of birth: 8/18/1978, Goldsboro, N. Carolina

Education:

Lehigh University, BS Geosciences 1997, graduated with honors, Bethlehem, PA 18015. *Thesis:* " Kinematic and temporal analysis of faults within the Smiley Creek Conglomerate, White Knob Mountains, southcentral Idaho" advisor: David Anastasio

Field Experience:

Undergraduate Field Camp, Lehigh University, 1999. Multiple day projects in S. Dakota, Wyoming, Idaho. 6 weeks total

Undergraduate senior thesis field work, 1999; collecting kinematic data on minor faults, field assistant to Diana Latta, paleomag. core drilling and extraction, White Knob Mtns., Idaho, 4 weeks

MS research, 2001; mapping of bedrock and surficial deposits, pedology, assembly and age determination of local quaternary stratigraphy, examination of quaternary faulting, 5 weeks.

EDMAP project, 2001; mapping of surficial and bedrock geology in the Dixon Mtn. 7.5 Minute Quadrangle for the USGS, Tendoy Mts. MT.

Field assistant in Mexico, 2002; structural measurements, collection of oriented paleomagnetic samples, mapping, 2 weeks.

Field Assistant on NSF Continental Dynamics project "*Tectonics of Indentor Corners*" in eastern Tibet, 2002; broadband seismic station deployment, maintenance, and collection, geochronologic sample collection, structural data collection, 6 weeks.

Additional MS research, 2002; regional scale landscape evolution investigation, mapping and correlation of river terraces, determination of local river terrace and quaternary stratigraphy, 4 weeks.

EDMAP project, 2002; mapping of surficial and bedrock geology in the Caboose Canyon 7.5 Minute Quadrangle the USGS, Tendoy Mts. MT.

Teaching experience:

Teaching Assistant, EES 21, Introduction to Planet Earth, 3 semesters

Teaching Assistant, EES 113, Life, Climate & the Rock Record. 1 semester

Teaching Assistant, EES 3, Global Environmental Change, 1 semester

Teaching Assistant, EES 341. Advanced Field Geology (field camp), 2 summers

Publications:

- Anastasio, D.J., Harkins, N.W., and Latta, D.K., 2002. Coeval in- and out- of sequence deformation within the Frontal Thrust Sheets of Tendoy Mountains, SW Montana. Abstracts with Programs – 54th Annual Geological Society of America Rocky Mountain Sectional Meeting.
- Harkins, N.W., Anastasio, D.J., Pazzaglia, F.J., and Latta, D.K., 2002. Neotectonics along the Red Rock Fault, SW Montana. Abstracts with Programs – 54th Annual Geological Society of America Rocky Mountain Sectional Meeting.
- Harkins, N.W., Latta, D.K., Anastasio, D.J., and Bartholomew, M.J., 2002. Surficial and Bedrock Geologic Map of the Dixon Mountain 7.5 Minute Quadrangle, MBMG/USGS Open File Report.
- Harkins, N.W., Anastasio, D.J., and Pazzaglia, F.J., 2003. Tectonic geomorphology of the Red Rock fault, segmentation and recent rupture history in the northern arm of the Yellowstone Topographic Wake. Geological Society of America Bulletin, in review.
- Harkins, N.W., Newton, M.L., and Anastasio, D.J., 2003. Geologic map of the Caboose Canyon 7.5 Minute Quadrangle, SW Montana, MBMG/USGS Open File Report (in prep).
- Latta, D.K., Anastasio, D.J., Harkins, N., Schmitt, J., and Aschoff, J. 2003. Out of sequence emergent thrusting during the early Tertiary, within the Sevier hinterland, Montana Recess, southcentral Idaho. Tectonics (in prep).

Grants Received:

- 2001- AAPG Grants-in-Aid – M.S. thesis work
Palmer Fellowship Award – M.S. work
- 2002 – USGS EDMAP/Statemap program – M.S. work

Honors, Awards, and Special Accomplishments:

- Bausch and Lomb Science Award, 1995
Chris Poster Memorial Scholarship, 1996
Lehigh University Education Grant, 1996-1997
Lehigh University Dean's List, 1996-1997, 1999-2000
Eagle Scout Award, 1997
Scholar Athlete Award, 1998, 1999
Varsity Co-Captain (Cross-country & Track) 1999-2000

**END OF
TITLE**